Structural studies and polymorphism in amorphous solids and liquids at high pressure

Wilding, Martin C.; Wilson, Mark; McMillan, Paul F.

Published in:
Chemical Society Reviews

DOI:
10.1039/b517775h

Publication date:
2006

Citation for published version (APA):
Wilding, M. C., Wilson, M., & McMillan, P. F. (2006). Structural studies and polymorphism in amorphous solids and liquids at high pressure. *Chemical Society Reviews*, *35*(10), 964-986. https://doi.org/10.1039/b517775h

Structural studies and polymorphism in amorphous solids and liquids at high pressure

Martin C. Wilding,[a] Mark Wilson[b] and Paul F. McMillan[bc]

Received 19th July 2006
First published as an Advance Article on the web 30th August 2006
DOI: 10.1039/b517775h

When amorphous materials are compressed their structures are expected to change in response to densification. In some cases, the changes in amorphous structure can be discontinuous and they can even have the character of first-order phase transitions. This is a phenomenon referred to as polyamorphism. Most evidence for polyamorphic transitions between low and high density liquids or analogous transformations between amorphous forms of the same substance to date has been indirect and based on the changes in thermodynamic and other structure-related properties with pressure. Recent studies using advanced X-ray and neutron scattering methods combined with molecular dynamics simulations are now revealing the details of structural changes in polyamorphic systems as a function of pressure. Various ''two state'' or ''two species'' models are used to understand the anomalous densification behaviour of liquids with melting curve maxima or regions of negative melting slope. Thermodynamic analysis of the two state model leads to the possibility of low- to high-density liquid transitions caused by differences in bulk thermodynamic properties between different amorphous forms and on the degree of cooperativity between low- and high-density structural configurations. The potential occurrence of first-order transitions between supercooled liquids is identified as a critical-like phenomenon. In this *tutorial review* we discuss the background to polyamorphism, incorporating the experimental observations, simulation studies and the two-state models. We also describe work carried on several systems that are considered to be polyamorphic.

Introduction

There have been many investigations of pressure-induced phase transitions and the associated structural changes. These investigations have revolutionised solid state chemistry and physics, geology and materials science, and are now being extended into biochemistry and biology. The studies have been enabled by dramatic advances in techniques in crystallography carried out *in situ* under high pressure conditions, both at X-ray synchrotrons and neutron scattering facilities and using

[a]*Institute of Mathematic and Physical Sciences, University of Wales at Aberystwyth, Ceredigion, SY23 3BZ, UK*
[b]*Department of Chemistry and Materials Chemistry Centre, Christopher Ingold Laboratories, University College London, 20 Gordon Street, London WC1H 0AJ, UK*
[c]*Royal Institution of Great Britain, Davy-Faraday Research Laboratory, 21 Albemarle Street, London W1X 4BS, UK*

Martin C. Wilding

Martin Wilding obtained his PhD in 1990 from the University of Edinburgh. He then studied glass relaxation at Lancaster University and at the Bayerisches Forshunginstitut für Experimentelle Geochemie und Geophysik, Bayreuth before moving to the US. He worked in the Thermo-chemistry Facility at Princeton University and subsequently at the University of California at Davis. Between 1999 and 2001 he visited Arizona State University where he worked closely with Prof. Paul McMillan on liquid–liquid transitions, a collaboration that continues in his current position as lecturer in Materials Physics at the University of Wales, Aberystwyth.

Mark Wilson

Mark Wilson was born in Derby. He obtained a BA from Oxford in 1991 and his DPhil (supervised by Professor Paul Madden) in 1994. He spent two years at the Max-Planck-Institut fuer Metallforschung in Stuttgart as an Alexander von Humboldt fellow. He returned to the UK in 1996 to take up a Royal Society University Research Fellowship, initially in Oxford, but later at University College London. He is presently a Reader in Computational and Physical Chemistry at UCL.

laboratory X-ray sources. High-pressure crystallography is carried out to megabar pressures in the diamond anvil cell (DAC) and in specially-designed large volume devices such as the Paris–Edinburgh toroidal apparatus. These new techniques and apparatus have also resulted in renewed interest in studying the structural changes in amorphous solids and liquids at high pressure. This is partly driven by the need to understand recently-described phenomena such as polyamorphism and pressure-induced amorphisation. The experimental studies are combined with advanced computational techniques to gain a new understanding of the properties and structural chemistry of the amorphous state.

Structural studies of liquids and amorphous solids at high pressure

Liquid and amorphous structure

To begin with we should consider what is meant by the "structure" of amorphous solids and liquids, and we briefly describe the techniques that are used to obtain this information. Unlike crystalline solids, neither of these "disordered" states of matter possess the property of long-range periodicity.[1–3] Because of the translational symmetry in crystals, diffraction data are conveniently analysed using reciprocal space methods to determine the individual atomic positions. Various descriptions of the crystal structure are then expressed in terms of individual bond distances and coordination polyhedra. The absence of long-range order in amorphous solids and liquids means that sharp diffraction peaks do not occur. However, X-ray and neutron scattering studies and molecular dynamics (MD) simulations reveal structural correlations that deviate from that of a completely random arrangement of atoms, indicating the presence of some degree of local order. At the simplest level (Fig. 1), in which the system can reasonably be described in terms of the packing of atomistic hard spheres, local ordering (short range order – SRO) is imposed by packing requirements. A chosen atom effectively orders the nearest-neighbour atoms as they can only approach to approximately the same atom–atom separation (around an atomic diameter). As a result, the nearest-neighbour separations observed for systems in both the liquid and glassy states are generally comparable to those observed for the corresponding crystals. Furthermore, this packing allows for the definition of local coordination polyhedra, analogous to those obtained from the study of the crystalline polymorphs. In many systems longer-ranged structural correlations may be usefully considered in terms of how these polyhedra inter-link[4] (Fig. 2). The structure of typical glass-forming systems, such as SiO_2, $ZnCl_2$, $GeSe_2$ and $SiSe_2$, for example, can be understood in terms of linked MX_4 tetrahedra. SiO_2 may be considered as dominated by corner-linked units, whilst $SiSe_2$ is dominated by edge-sharing units. Both $ZnCl_2$ and $GeSe_2$ are "intermediate" with structures which can be considered as a mixture of corner- and edge-sharing units. The linkages formed by these units leads to the disordered states having order beyond the SRO imposed by the nearest-neighbour packing considerations. Such intermediate-range order (IRO) is observed directly in diffraction experiments as a "prepeak" or first-sharp diffraction peak (FSDP)[5,6] in the total scattering function and corresponds to density fluctuations on a 0.5–1.0 nm length-scale. In these systems the polyhedra link together (by a combination of corners and edges) to form complex units (chains, rings…). As shown in Fig. 2, the structure factors can be effectively decomposed into structural ranges. The FSDP effectively describes the inter-polyhedral linkages (IRO)[4,7–9] whilst the long-range oscillations correspond to the nearest-neighbour (tetrahedral) packing correlations. Above the system melting point the liquid structure can be considered as evolving *via* the continual breaking and formation of the metal–anion bonds. On average, however, the system may retain order (density fluctuations) on the intermediate length-scale in an analogous fashion to the retention of averaged SRO. The sharpness of the FSDP indicates correlation lengths which may extend out to 5 nm.[5,6] Furthermore, the presence of such IRO has been shown to have significant ramifications for glass formation

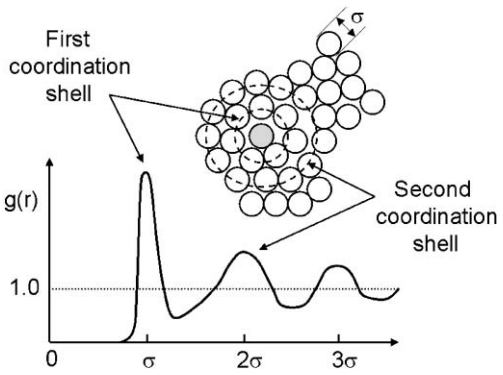

Fig. 1 Atomic configurations for a typical Lennard-Jones liquid of diameter σ showing the first and second coordination shell.[3,121] The pair distribution function shows peaks corresponding to the first and second coordination shells.

Paul F. McMillan

Paul F. McMillan is Professor of Chemistry at University College London and in the Davy-Faraday laboratory at the Royal Institution. He is also Director of the UCL Materials Chemistry Centre. He graduated with a BSc in Chemistry from Edinburgh University in 1977 and moved to Arizona State University for his PhD (1981). He became Professor there in 1992 and Director of the Centre for Solid State Science (1997). Since moving to London in 2000, he has established laboratories for developing solid state chemistry and new materials research under high pressure conditions, extending to biology and nanomaterials. He was awarded a Wolfson-Royal Society Research Merit Award (2001–2006) and an EPSRC Senior Research Fellowship (2006–2011). He was elected Fellow of the RSC and received the award for Solid State Chemistry (2003).

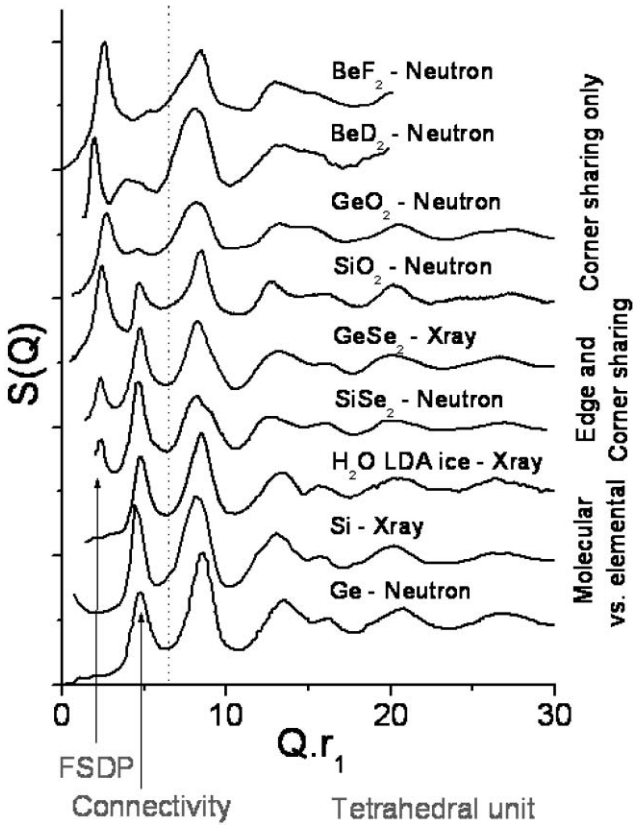

Fig. 2 Comparison of several tetrahedral glasses and amorphous materials, scaled by the first peak in $g(r)$, denoted r_1. The three structural ranges are denoted (I) tetrahedral unit, (II) connectivity and (III) first sharp diffraction peak (FSDP).[4]

from the cooled liquid state. The relaxation dynamics on the intermediate-ranged length-scale appear to slow dramatically compared with that associated with the short-range order.[10] As the liquid is cooled, therefore, the long-time (α) relaxation becomes dominated by density fluctuations on the intermediate-range length-scale.

A clear distinction exists between crystalline and amorphous structural data obtained from diffraction experiments. For crystalline samples, sharp (Bragg) features are observed whose origin lies in the presence of long range periodicity. For amorphous samples structural features are significantly broader reflecting the inherent structural disorder.[1–3] The disordered atomic environments also lead to broadening in the bands obtained by NMR, IR, Raman, X-ray, *etc.*, spectroscopy. Another important difference lies in the interpretation of amorphous and crystal structure data. For the crystal, unit cell models can be used to represent both the local and long-range structures, with the (ideal) infinite crystal lattices generated by the periodic replication of these (relatively simple) structural units. In reality the crystals contain defects and have surfaces, both of which are not accounted for by replicating an ideal unit cell. However, for low defect concentrations, these periodic methods are appropriate for the treatment of the experimental data. Only for massively disordered crystals or finite nanoparticles do the reciprocal space assumptions begin to break down. On the other hand, for amorphous solids and liquids, the long-range order is not present. Analysis of the structural correlations present in diffraction data (*i.e.*, the scattering function $S(Q)$) by Fourier transformation yields sets of spatially averaged inter-atomic distances, usually shown as the radial distribution function ($g(r)$), or in terms of pair correlation functions ($P(r)$). These give the probability of finding another atom at a distance r from each central atom, averaged over the entire sample and over time, and they are used to deduce average bond distances, angles, and coordination polyhedra within the glass or liquid. However, unlike the interpretation of crystal structure data, there is no longer any expected correspondence between local and long-range structures. The local structure obtained is averaged both over time and over the sample. For example, therefore, if there were different atom coordination environments in equilibrium in a given sample, then the observed rdf would be a weighted mean of contributions from these different environments. For systems which contain atoms of more than one chemical identity, then partial rdfs, $g_{\alpha\beta}(r)$, may be defined which give the probability of finding an atom β at a distance r from atom α. These functions contain additional information. Coordination numbers may be obtained by integrating the first peak (although, for liquids in particular, this may be difficult as there will be atom diffusion between shells). In addition, if the partial rdfs are available, then the geometries of the local coordination polyhedra may be surmised.

Liquids, supercooled liquids and glasses

Liquids, like amorphous materials also lack the internal order that characterises crystals and can continually relax on an observable timescale in response to temperature or pressure. Liquids are distinguished from amorphous materials such as glasses on the basis of this relaxation process. When a liquid is cooled below the crystallisation temperature the ability for the structure to relax to an equilibrium configuration in this super-cooled regime is lost as the structural relaxation time increases.[1–3,11–13] Eventually, a glass can be formed distinguished by a glass transition temperature. Glasses are not in thermodynamic equilibrium but reflect the partial relaxation of structural configurations in the super-cooled liquid, they are therefore metastable and reflect neither snapshots of the stable liquid nor disordered forms of chemically equivalent crystalline phases.

Amorphous solids can be formed through a variety of routes, not just formation by super-cooling stable liquids. These include chemical vapour deposition onto cold substrates and pressure induced amorphisation,[14,15] a process that can be viewed as metastable melting. The structures of amorphous materials can change with pressure and different structures can be produced by different routes;[16] such structural changes are reflected in the macroscopic properties of amorphous phases such as their volume and enthalpy and in some cases, the changes in structure are abrupt and occur over a narrow interval of pressure or temperature. Amorphous solids should be regarded as being inherently ''polyamorphic'', there can be differences in short- and intermediate range order for amorphous solids produced at different pressures and temperatures.[17,18]

A useful generalised structural description of the amorphous state is that of the ''configurational landscape'',[19] that can be

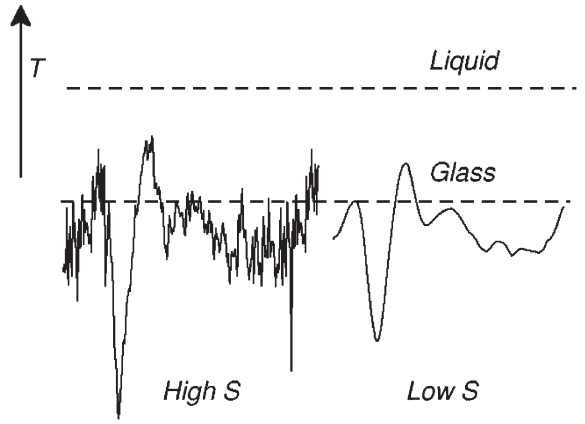

Fig. 3 A schematic simple energy landscape. The panel on the left has many local energy minima (with a corresponding high entropy) whilst the right-hand landscape is relatively smooth (low entropy). Above the melting point all energy minima are energetically accessible. Below the glass transition temperature movement between local energy minima is kinetically controlled.

depicted as a multi-dimensional plot of the potential energy developed for a particular local and long-range arrangement of atoms and bonds (*i.e.*, a ''configuration'') (Fig. 3). The resulting concept is often displayed as two- or three-dimensional plot of energy (E) *vs.* the generalised configurational coordinate(s), ζ. A crystal corresponds to a single point in ζ (*i.e.*, to one particular arrangement of the atoms and bonding), with a very low energy. The remainder of the peaks and valleys in $E(\zeta)$ constitute the ''landscape'' of amorphous configurations. The density of potential wells in $E(\zeta)$, or the number of possible alternate possibilities for the SRO/IRO, determines the configurational entropy ($S_{conf}(T)$). In a liquid or supercooled liquid, all of the individual potential wells are occupied according to Boltzmann statistics: the amorphous system is in a state of internal thermal equilibrium. As the temperature is decreased, barriers in $E(\zeta)$ begin to poke as mountains and ridges above the sea of thermal excitation, and valleys and potential wells become isolated from each other: the system has fallen out of internal thermal equilibrium and has become ''non-ergodic'' in that time- and space-averages of thermodynamic properties are no longer equivalent. The temperature-cooling rate range over which this occurs is termed the ''glass transformation range''. An even more useful description has been recently developed, in which a ''branching tree'' approach is used to describe the configurational energy minima and the barriers between them.[19]

Crystalline phases exhibit polymorphic transitions as a function of pressure and temperature, where different packing schemes are stabilised under different density–entropy conditions. The P–T range of the phase transitions are determined by the relative energetics of the two structural arrangements. The first-order *vs.* 2nd- or higher-order nature of such thermodynamic transitions is determined by the lack or presence of connectivity between the minimia in the $E(\zeta)$ landscape, and the transformation kinetics are fixed by the effective barrier heights and transformation pathways between the two phases. In the case of amorphous materials, high energy barriers can develop between different regions of the available configurational energy landscape, resulting in the possibility of first-order like phase transitions between amorphous states with different SRO/IRO structural types and thermodynamic properties, that are analogous to the crystal–crystal transitions. Such behaviour is termed ''polyamorphism''. Because the number, type and relative potential energy depths and barrier heights between and among various amorphous configurations varies as a function of pressure, it is expected that polyamorphic transitions are likely to be encountered as the full range of pressure–temperature space is explored.[20]

The terminology used to describe changes in structure between amorphous solids is misleading. It is incorrect for example to describe a glass as a metastable phase. A phase is strictly a macroscopically homogeneous equilibrium stable state and an amorphous solid cannot be described unambiguously as a thermodynamic phase. The evolution of metastable states should be viewed within a definite timescale in a ''configurational space'', and so phase transitions should therefore not be possible between different amorphous and non-ergodic phases.[1,12,19,21–23] There are no thermodynamic restrictions on the transition between liquids or liquid crystals and the overturn of the P–T melting curves in systems such as SiO_2, Se, S and P are regarded as evidence for potential first order transitions between different liquid phases.[18,24–26] The order parameters for these transitions are density and entropy, as in liquid–gas transitions and in a similar way, lines of transitions between high- (HDL) and low- density (LDL) liquids are terminated by critical points.

High pressure liquid behaviour and LDL–HDL transitions

Abrupt changes in macroscopic properties

Liquid structures can change when compressed. The changes in liquid and amorphous materials structure can be determined by direct measurements of the averaged structure by neutron or X-ray diffraction and through measurement of structure-related properties such as electrical and thermodynamic properties. Transitions between high and low-density liquids have been observed in the stable liquid regime for liquid phosphorus.[25,27,28] In systems where LDL–HDL transitions have been suggested however, the transition occurs below the stable melting curve.[20] This means that transitions between different structured liquids can only be observed if the liquids are super cooled sufficiently. Candidate polyamorphic systems are identified through study of their melting relations as a function of the pressure. It is generally expected that the slopes of melting curves, dT_m/dP should be positive as indicated by the Clausius–Clapeyron relation:

$$\frac{dT_m}{dP} = \frac{\Delta V_m}{\Delta S_m} = \frac{V_{liquid} - V_{crystal}}{S_{liquid} - S_{crystal}} \quad (1)$$

Liquids are less ordered than the corresponding crystal, so that ΔS_m is always positive. Melting is usually associated with an increase in volume (positive ΔV_m). However, many simple systems show a negative melting slope and there can be one or more maxima in the melting curves. Perhaps the best known

compound with a negative initial melting slope is H_2O (from the ice Ih phase),[29] as discussed below. Cs, Ba, Eu, Pu, Si and Ge also have negative dT_m/dP slopes to the melting curve.[30] Si and Ge are of additional interest in that a maximum to the melting curve is expected at negative pressure. Direct analogy with gaseous and liquid systems indicates that the density is the state variable believed responsible for liquid–liquid and amorphous–amorphous transitions. The accompanying structural changes are expected to be changes in short-range (*i.e.* coordination number) or intermediate range length-scale (topology). In such cases fluctuations in density might be anticipated in the (high temperature) stable liquid, reflecting the presence of more than one polyamorphic form below the liquid freezing point.

In amorphous solids changes in structure are complicated because of the metastable and non-ergodic nature of these materials. Transitions between different forms require that the energetic barriers to transition between metastable forms should be lower than those for transition between stable phases. The existence of transitions in glasses is widely supported by experimental studies but lack the characteristic requirement for first order transitions, that is, a zero transition width. Experimental evidence indicates the transition width can be non-zero with unusual kinetics.

High pressure studies of liquid and amorphous structure are therefore crucial in identifying systems that may be candidates for liquid–liquid and amorphous–amorphous transitions. Such transitions may involve changes in volume, enthalpy and entropy (ΔV, ΔH and ΔS) and, if volume changes are small, the transitions can be intercepted at relatively low pressures or even under ambient pressure conditions. *In situ* observation of polyamorphic changes is difficult, involving high temperature, if the stable liquids are to be observed. Furthermore, supercooling and quenching high pressure liquids to a glass is also experimentally difficult and the high pressure amorphous phases may not be recoverable. Extensive studies using toroid-type pressure cells, which can generate pressures to 0.3–13 GPa and temperatures of up to 2000 K, have suggested the occurrence of phase transitions in elemental liquids such as Se, S, Te, I_2 and P,[24,31] as well as in As_2Se_3, As_2S_3 and Mg_3Bi_2.[32] These liquids show abrupt changes in the electrical conductivity of the stable liquids analogous to those associated with insulator–semiconductor-metal transitions in crystalline solids. These changes are associated with volumetric changes, $\Delta V/V \sim 0.5\%$ and viscosity changes, inferred from the quenching behaviour of melts under pressure.[27,33] In liquid selenium, for example the electrical conductivity of the liquid increases by two orders of magnitude at pressures of approximately 4GPa within a transition width of 0.3 GPa.[27,33] Changes in the properties of liquid sulfur are reported at 8 and 12 GPa. At 8 GPa there is a change in volume while at 12 GPa there is an increase in electrical conductivity of 1–2 orders of magnitude, consistent with a change from a semiconductor to metallic liquid. In both selenium and sulfur the location of the changes in electrical properties depend on the rate of change of pressure and temperature, this hysteresis resulting in apparent regions of coexistence of different liquid states. Like selenium, liquid phosphorus shows an increase in electrical conductivity consistent with a semiconductor to metal transition, accompanied by a decrease in liquid viscosity. These transformations are coincident with a volume change of $\Delta V/V$ of 40%.[25,28,34] The abrupt transformation in phosphorus may result from the same mechanism that causes bonding changes in equivalent crystalline polymorphs. As such density ordering is suggested as a mechanism for a transition between different phosphorus liquids. Direct observation of such a transition in phosphorus has been reported by Katayama.[25,28]

The work by Brazhkin[27] and others has shown that the abrupt transition in electrical conductivity and boundaries between semiconductor and metallic liquids are associated with changes in the slope of the melting curves, dP/dT. This means that in the stable liquids the changes in electronic properties correspond to changes in density. The transitions between liquids can occur over 0.3 to 0.5 GPa, but can be more abrupt, for example over a range of 0.01 GPa for phosphorus. The boundaries in these transition regions show negative Clapeyron (dP/dT) slopes which means that the entropy of the denser, metallic liquids is higher. A possibility is therefore raised that stable liquids can undergo transitions from one stable liquid phase to another with density and entropy as the order parameters. The mechanisms for such transitions are elusive (electrical conductivity measurements are not a direct probe of the liquid structure) and there may be fluctuating micro- and nano-scale domains as well as regions of coexistence of the high- and low-density liquids. As such the apparent transition between one liquid and another occurs over an interval of pressure and can be interpreted as critical-like fluctuations, a critical-like point occurring at lower temperature in the supercooled liquid regime. In the case of liquid phosphorus however, X-ray scattering and radiography describe a liquid–liquid transition between low-density (LDL) and high-density (HDL) stable liquid phases at $\sim$1 GPa and $\sim$1000 K.

High pressure experimental techniques

The study of liquid and amorphous material behaviour under conditions of high pressure is a highly interdisciplinary field. The changes in physical properties with pressure are of interest to inorganic and organic chemists, mineralogists and solid state physicists. Interest in this field of study, following the pioneering work of Bridgman, has increasingly developed following the observed changes in physical properties and behaviour of the materials under pressure.[35] Studies of crystal structure have been performed *in situ* up to pressures of 1–2 Mbar, and the results used to interpret changes in properties such as electrical conductivity and magnetism, and to establish the phase equilibrium between different crystalline phases. There have been fewer studies of liquids and amorphous solids, and the interpretation of the results is less direct.

In situ studies of materials at high pressure involve two approaches. Optical and spectroscopic experiments can be carried out with high pressure cells made using materials such as silica glass, sapphire and diamond. These are so-called ''windowed'' experiments where the windowed material is ideally transparent to optical and infrared radiation and is also resistant to the high pressures and temperatures required for *in situ* study. Of most importance is the diamond anvil cell

(DAC). In the DAC the sample is placed between the flattened tips of two gem quality single crystal diamonds and contained within a hole drilled in a gasket (usually made of metal). The sample chamber is brought to high pressure by applying mechanical force to the diamonds. High temperatures can be generated by resistance heating or laser heating. Diamond is transparent to radiation over a wide range of the electromagnetic spectrum, and various optical spectroscopy experiments to probe crystal and glass structures at high pressures in the DAC have been carried out. Substantial X-ray transmission occurs above 112 keV, so that X-ray diffraction and amorphous scattering experiments can be most readily carried out at X-ray synchrotron radiation sources. However the sample chamber and the sample size are generally very small (on the order of 50–200 μm in diameter), depending upon the pressure range to be investigated, and substantial thermal gradients can exist. Several studies of amorphous solids, including glasses, have been carried out using synchrotron X-ray scattering methods; however, *in situ* studies of liquid structure under combined high-P,T conditions are generally difficult to achieve.

An alternative experimental approach is the use of "large volume" presses equipped with multi- or toroidal type anvils. These are not transparent to visible, infrared or ultraviolet radiation, and so optical spectroscopy experiments are not permitted. In addition, the sample assemblies absorb X-rays. In some configurations, using low absorbing sample containers or pressure-transmitting assemblies, *in situ* diffraction data can be obtained. A major advantage of the multi-anvil or toroidal anvil pressure devices for liquid studies is that sample volumes are much larger than in the DAC, and the thermal regime is much more easily controlled. In addition, simultaneous *in situ* measurements of physical properties such as electrical conductivity and liquid viscosity can be made. However, certain special requirements must be met if liquid and amorphous structures are to be measured. One type of toroidal cell has been used extensively in high pressure research by Russian groups and also by groups from Paris and Edinburgh, in a cell that was specially designed for neutron crystallography.[36,37] This design utilises low- or null scattering gasket material and allows diffraction data of low scattering materials such as liquids and glasses to be obtained to high values of the scattering vector (Q).

Neutron and X-ray diffraction studies of liquids and amorphous solids

Liquids and amorphous materials show changes in structure and associated bulk macroscopic properties as a function of composition, pressure and temperature. Neutron and X-ray diffraction experiments offer the opportunity of investigating the microscopic structure of stable and metastable liquids and also amorphous materials.[8,9] Neutrons may be sensitive to light elements, particularly hydrogen, and so aqueous solutions and ice structures can also be studied. Neutron scattering can provide a direct measure of nuclear arrangements over a wide range of length scales. Thermal and high energy neutrons are highly penetrating and a powerful bulk probe, which can provide high resolution information at the atomic level which is needed for the study of liquid structures. With the development of third generation synchrotron sources, there has recently been huge progress in producing instrumentation for using highly penetrating X-rays of $\sim$100 keV[38] for the study of liquid and glass structure. These high energy X-rays act as a bulk probe and cover a wide Q-range, up to 25 $Å^{-1}$, comparable to that of neutron instruments at spallation sources. Neutron and high energy X-ray diffraction can be viewed as complementary techniques and are particularly useful for studying oxide or hydrogenous systems, as, while neutron scattering lengths vary erratically across the periodic table, X-ray form factors vary as a function of atomic number. Other spectroscopic techniques such as Extended X-ray Absorption Fine Structure (EXAFS)[39] are also element specific and act as a local structural probe, EXAFS is restricted however to high Q values although is sensitive to low concentrations of the element being studied, and the results can be very effectively combined with diffraction techniques.[40] Generally one of the goals of the study of liquid and glass structures is an attempt to link the bulk macroscopic properties to the microscopic structure.[41]

Raman spectroscopy can be used to probe the vibrational structure of liquid and glassy systems. These spectra may show specific structure in the form of distinct bands at specific frequencies. These modes may then be assigned to normal modes of vibration of the local coordination complex.[42]

High pressure neutron diffraction studies are carried out using the Paris–Edinburgh type press.[37,43] Pressure is usually generated by two opposed toroidal anvils, made of tungsten carbide or sintered diamond, that deform a metal gasket (usually TiZr). Incident neutrons can be directed down the compression axis with scattered neutrons or X-rays detected in the plane of the gasket. The anvils themselves can be coated with boron nitride to act as collimators in this latter configuration although there can still be contributions from the anvils, which are often hard to subtract because the anvils deform when compressed. Since the anvils close on compression, typically from 1.6 mm to 0.8 mm at 5 GPa for a TiZr gasket, the scattered signal decreases significantly with increasing pressure. Several notable studies have been completed including studies of amorphous ices and GeO_2.[44,45] More recently studies have been completed on Mg-silicate glasses and vitreous B_2O_3.

A historically important model for understanding glass structure is the continuous random network (CRN) in which a random structure is generated by systematically linking the appropriate short-range structural units.[6,46,47] However, diffraction studies indicate that the glass structures are more ordered than the CRN models would suggest.[48] As a result, although modified random network models form a good basis for interpreting diffraction data, full interpretation is difficult without additional input. It is common, therefore, to combine neutron results with other data such as X-ray, spectroscopy, NMR and thermodynamic property data. Diffraction modelling techniques such as Reverse Monte Carlo[49] and Empirical Potential Structure Refinement[50] (EPSR) have been developed in recent years to fit model structures of glasses and liquid diffraction data, in an attempt to provide an analogy to the

modelling crystalline powder patterns with Rietveld refinement methods.

Simulation studies of liquids, glasses and amorphous solids

The computer simulation of liquids and amorphous solids has a long history.[51] In atomistic models the system properties are decomposed into terms which depend on the atom coordinates $\{\mathbf{R}_i\}$. As a result, the internal energy, $U(\{\mathbf{R}_i\})$, may be calculated and used to obtain the forces acting on each atom. These forces can then be used within a Newtonian mechanics scheme to generate atom positions and velocities as a function of time (molecular dynamics). MD simulations can be performed within a number of ensembles. At the simplest level the total system energy is a conserved variable (NVE ensemble). More usefully for promoting direct contact with experimental investigations, constant temperature (NVT ensemble) can be maintained *via* the application of thermostats, in which the temperature is maintained in the simulation cell *via* energy transfer with a connected heat bath. Analogous techniques can be applied to allow for constant pressure simulations (NPT ensemble) in which barostats control the simulation cell volume in order to maintain the required pressure.

At the simplest level $U(\{\mathbf{R}_i\})$ may be approximated as a sum of purely pair-wise additive energy expressions, $U(\{\mathbf{R}_i\}) = \sum_{i,j} U_{ij}(r_{ij})$, where r_{ij} is the separation between atoms i and j. Potentials obtained using these approximations are termed effective pair potentials (EPP) as they may implicitly incorporate many-body effects (in contrast with true pair potentials which account only for the interaction of a pair of atoms). The parameters which control the EPPs can be obtained by reference to experimental observations (thermodynamics, diffraction patterns, mechanical properties). However, a relative lack of experimental information may hinder the extraction of unambiguous parameter sets, with the result that individual parameters may lose their physical meaning. A consequence of this loss of meaning may be a reduction in the transferability of the potential model between state points, compositions or even different materials.

In theory, therefore, simulation methodologies are ideal in order to make direct contact with experimental investigations. Thermodynamic properties, which may depend on both the atom positions and velocities, can be calculated as these are known unambiguously. Free energy calculations, however, are more problematic as the system entropy is not purely a function of position and velocity. In these cases approximations may be sought in order to calculate the vibrational contribution to the entropy, or entropy differences may be calculated by reference to a known ideal system (thermodynamic integration). Direct contact may be made with (neutron or X-ray) diffraction experiments. The atomic structure factors, $S(\mathbf{k})$, can be calculated from the known atomic coordinates ($S(\mathbf{k}) = \langle A^*(\mathbf{k}).A(\mathbf{k})\rangle$, where $A(\mathbf{k})$ is the Fourier component). Furthermore, for mixtures of atoms the *partial* structure factors, $S_{\alpha\beta}(\mathbf{k})$, may be obtained allowing the total structure factors to be constructed. In order to generate the corresponding X-ray function the coherent neutron scattering lengths are replaced by the (k-dependent) form factor functions. As a result, the functions obtained from the simulation studies contrast with those obtained experimentally. In the simulation studies the partial functions are obtained with relative ease from a knowledge of the atomic coordinates but must be combined (with a knowledge of the appropriate neutron scattering lengths or X-ray form factors) to give the total scattering functions (which allows for direct comparison with single scattering experiments). For experimental studies the partial structure factor information is relatively difficult to obtain. Isotopic substitution and neutron diffraction can yield such information but even these techniques are limited to systems for which stable isotopes with significantly different neutron scattering lengths are available. Partial structure factor information may also be extracted by exploiting isomorphous materials.[8]

In order to study liquid state and, in particular, glassy systems the simulation time- and length- scales available must be maximised. Pseudo-bulk environments are generated by periodically replicating a central cell (and hence removing the surfaces and creating a pseudo-crystalline system with a large unit cell). However, the central simulation cell must be large enough to accommodate the structural correlations inherent in the system of interest (which may be significant in systems which have significant structural ordering beyond that imposed by the short-range packing effects). The available simulation time-scales are controlled by the requirement to accurately integrate the Newtonian equations of motion in order to track atomic trajectories. This requirement effectively limits the usable integration time-step (the real time increment from a single MD step) to around 10^{-15}s. As a result, therefore, atomistic simulations are limited to time-scales of the order of nanoseconds. Electronic structure methods, in which the electron density is explicitly accounted for and hence which offer a potentially greater level of accuracy, generally require a significantly greater computational effort and, as a result, the affordable length- and time-scales are typically shorter. The issue of accessible time-scales becomes even more significant when considering simulation methodologies to probe the supercooled state. Under experimental conditions glasses may be formed from the liquid state by rapid cooling. However, the maximum accessible cooling rates are still of the order of 10^{10}Ks^{-1}. For simulations, however, even the slowest accessible cooling rates are orders of magnitude faster. As a result, direct comparison between the glassy states accessed by both experimental and computational techniques, remains difficult. An alternative strategy, employed for example to access the glassy state for silicon, is to modify the potential model in order to access glassy structures. Luedtke and Landman, for example, utilise a modified Stillinger–Weber potential to enforce a larger number of tetrahedra observed in the glassy state of silicon.[52] The unmodified Stillinger–Weber potential is unable to access these states from the supercooled liquid on the simulation time-scales.

An alternative to attempting to access the low temperature glass structures themselves is to identify signatures of polyamoprhic behaviour in the liquid state. Both mixtures of Al_2O_3/Y_2O_3[53] and liquid Si[54] show significant density fluctuations above their respective melting points indicative of the presence of low and high density structural units.

The thermodynamic case for LDL–HDL transitions

Pressure-induced amorphisation

Liquid–liquid phase transitions that occur at constant composition represent a minimisation of the free energy in response to the pressure or temperature. There are density and entropy differences between the amorphous forms and, in the case of stable or metastable (supercooled) liquids, the polyamorphic transitions constitute true thermodynamic transformations of the first order between systems that are in internal thermal equilibrium. For polyamorphism within glasses and other non-ergodic amorphous states, the transformations recorded as a function of the applied pressure or temperature appear as changes in the structure or properties over a narrow interval of pressure and temperature. For example, polyamorphism is reported to occur in SiO_2 and GeO_2 glasses.[15,18,26,44,45] Such changes in the glassy or non-ergodic amorphous state might indicate the presence of a liquid–liquid transition in the supercooled regime.

For systems with a negative Clausius–Clapeyron relation, the negative melting slopes of materials under pressure have important implications for the behaviour of low pressure crystalline polymorphs. Metastable extensions of the melting curves can be intercepted and an amorphous material produced irreversibly. This is pressure-induced amorphisation. This was reported by Mishima for H_2O, when ice Ih was compressed and the "melting line" crossed.[29] The amorphous H_2O produced by pressure-induced amorphisation is a structurally distinct form of amorphous ice (termed high density amorphous ice; HDA), with a higher density than the amorphous forms of ice produced, for example, by condensation from vapour (low density amorphous ice; LDA). In more complicated phase diagrams, such as SiO_2, the melting curves do not necessarily become negative but show incipient maxima in the melting curve that are intercepted by polymorphic crystal–crystal transitions. The high pressure crystalline phase may have a different dT_m/dP curve and intercept at a triple point. If the melting curve for the lower pressure crystalline polymorphs is extrapolated then these too can form metastable melting curves which are intercepted and pressure-induced amorphisation can occur.

Pressure-induced amorphisation[55] can be considered in terms of metastable melting. In stable melting, the transformation between crystalline and liquid phases occurs when the Gibbs free energies of the two phases are equal. In the metastable case, melting (amorphisation) will likewise occur when the Gibbs free energies of the crystal and extrapolated liquid phase are equal. A solid amorphous material results with thermodynamic properties such as volume, enthalpy and entropy that can be mapped onto a non-crystalline state that is in a state of metastable thermodynamic equilibrium. Metastable melting is used to suggest a mechanism for pressure induced amorphisation. As low pressure, low density crystalline phases are compressed equilibrium structural changes include changes in short range order such as changes in coordination number. Potential energy barriers must be overcome for the low density crystalline phase to transform to the stable high density crystalline states. If there is sufficient thermal energy to overcome barriers to intermediate metastable states then amorphous forms can be produced. These intermediate states will not be crystalline and there may be several intermediate states separated by low potential energy barriers, each accessed by thermal motion. This series of related amorphous states or energy landscape is similar to that produced by quenching a supercooled liquid to a glass; the exact structural configuration is a reflection of the relaxation history, *i.e.* thermally activated jumps between closely related metastable, non-crystalline states.

One of the most important results from the study of pressure induced amorphisation of simple crystalline substances is that the amorphous forms produced have macroscopic thermodynamic properties that are different from amorphous materials produced at lower pressure (ΔV, ΔH and ΔS). This is the origin of the term polyamorphism; different amorphous forms of the same substance can be produced by different pressure–temperature routes. From thermodynamic arguments, the Gibbs free energy of these amorphous forms will have a different pressure and temperature dependence and there may be a transition between the amorphous forms of the same material. This may be continuous or discontinuous and may be indicative of a first-order transition between liquids in the supercooled regime. The close relation between pressure induced amorphisation and changes in the structure of amorphous states implies, in a one-component system, that there are differences in density in the liquid. The presence of two species and differences in density and entropy between them can be used to construct two-state models for phase transitions that are analogous to liquid–gas transitions.

Two state models

Two state models were developed from the late 1950's onwards to explain the unexpectedly complex melting curves observed at high pressure for substances such as Rb, Cs, Te, Ba and Eu.[30,56] These systems display maxima in their melting curves which may be attributed to the presence of different local environments in the liquid state. Since there is a change in dT_m/dP slope and potential to extrapolate the metastable extension of the melting curve to low temperatures there is an immediate connection between this type of model and pressure-induced amorphisation. In Fig. 4a, the phase diagram of H_2O is shown schematically, together with the reported stability fields of two amorphous forms of ice, LDA and HDA, as can be seen, the metastable extension of the ice Ih melting curve can be intercepted when ice Ih is compressed at low temperature. The amorphous form of ice produced is HDA and is formed beyond the spinodal limit to LDA.[29,57,58]

The entropy of a liquid is greater than that of equivalent solid phases. This means that changes in dT_m/dP slope reflect a change in density through the Clausius–Clapeyron relation. In a one component system, the increased density of the liquid is assumed to reflect the presence of a high density liquid species. High and low density species exist in the stable liquid, according to the two-state model and the relative proportion of each varies as a function of pressure and temperature. In the original versions of the two state model, developed by

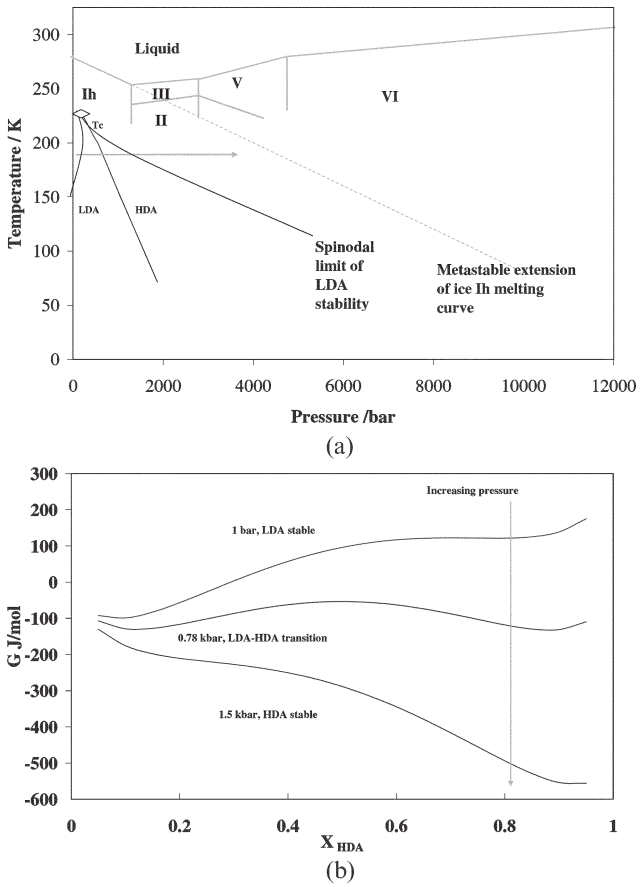

Fig. 4 a. Phase diagram for water showing the negative dT_m/dP curve for ice Ih. Superimposed on this diagram is the critical point and line of LDA–HDA transitions calculated form the two state model of Ponyatovsky and others.[60] The two spinoidal lines represent the stability limits of the two amorphous forms of ice. The arrow indicates an isothermal compression of LDA (the corresponding changes in Gibbs free energy are shown in Fig. 4b). b. Gibbs free energy calculated from the two state model of Ponyatovsky[60] showing the stable fraction of the low- and high-density amorphous forms as a function of mole fraction of the HAD component. The curves displayed from top to bottom represent the effect of increasing the pressure. The pressure trajectory is that shown in Fig. 3a

Rapaport,[30,56] the high and low-density melt species were assumed to be domains with local packing (short-range order) similar to those in high- and low-pressure crystal polymorphs. The increase in liquid density, evidenced by the overturn in melting curve, is a reflection of the increased abundance of the high-density species.

The arbitrary high- and low-density species in the two-state model are treated as thermodynamic components. The equilibrium fraction of each species is a function of pressure and temperature and reflects the minimisation of free energy. Rapaport applied the regular solution mixing model of Guggenheim[59] to the liquid, for a low density species (A) and a high density species (B) the equilibrium molar free energy for the liquid is defined by.

$$G = X_A G_A + X_B G_B \quad (2)$$

With X_A and X_B the mole fractions of the low- and high-density species. The partial molar free energy of each species is defined in terms of the specific volume contribution:

$$\begin{aligned} G_A &= G_A^0 + V_A^0(P - P_0) + RT\ln(X_A) + W(1 - X_A)^2 G_B \\ &= G_B^0 + V_B^0(P - P_0) + RT\ln(X_B) + W(1 - X_B)^2 \end{aligned} \quad (3)$$

Here G_A^0 and G_B^0 are the standard state molar free energies associated with the low- and high-density liquid species. The standard state molar volumes are V_A^0 and V_B^0 respectively. The standard state pressure is P_0 and the absolute temperature is T. R the universal gas constant. W is the regular solution interaction parameter. The total molar free energy of the liquid is:

$$\begin{aligned} G = X_A(H_A - TS_A) + (1 - X_A)(H_B - TS_B) + \\ P[X_A V_A + (1 - X_A)V_B] + RT[X_A \ln X_A + \\ (1 - X_A)\ln(1 - X_A)] + X_A(1 - X_A)W \end{aligned} \quad (4)$$

The regular solution interaction parameter W will be non-zero if there is a mixing contribution to the excess enthalpy of the liquid. This parameter is the key to interpreting liquid–liquid transitions in terms of the two-state model. In Rapaport's model a non-zero value of W can be thought of as reflecting the direct interface energy between two structural species, or more generally as a contribution from the cooperativity of bonding arrangements if anomalous changes in bonding or coordination occur as a function of density.

One consequence of the non-ideal interaction parameters is that a second critical point (in addition to that terminating the liquid–gas boiling curve, and as shown in Fig. 4a) can be defined according to.

$$T_c = \frac{W}{2R} \quad (5)$$

The consequence of this formalism is seen when the temperature is decreased. The equilibrium concentration of each species will vary as a function of pressure and temperature. At high temperatures, in the stable liquid, the change in species abundance is a smoothly varying function of pressure and at higher pressures a single phase liquid with an increased abundance of the high-density species is stable. This single phase liquid is stable at temperatures above the second critical point, but in the supercooled regime it is possible for sub-critical behaviour to be encountered. This can be illustrated by considering the minimisation of free energy. Fig. 4b shows the behaviour of the liquid free energy as a function of pressure from the modified two-state model of Ponyatovsky.[60] These functions show a series of minima with the minima associated with an excess of the HDA state becoming more favourable as the pressure is increased. As a result, as the pressure is increased, there will be a gradual increase in the abundance of the high density species as the higher pressure liquid will have an increased density and, because of the differences in entropy and enthalpy between different species, different thermodynamic properties. At lower temperatures the variation in abundance of the high density species is less smooth. This would be the regime of "critical like" fluctuations observed by Brazhkin and co-workers.[27] At lower temperatures still a transition between two

(super-cooled) liquids occurs (Fig. 3b). There are two spinodal lines defined in the subcritical region, these mark the extreme limits of stability of the two species. Transitions between liquids dominated by high and low-density species can occur in the supercooled region, above the calorimetric glass transition. If low pressure glasses or amorphous materials are compressed then an amorphous form with lower free energy could be accessed provided there was a relaxation process (thermally activated jumps) allowing these more stable structural configurations to be achieved. This would be equivalent to a glass quenched from the supercooled high pressure liquid. The two-state models described above have been used with success in describing the stability fields of different amorphous forms of water.[61] In addition these types of model can be used to describe the anomalous thermodynamic properties of water, including anomalous contributions to volume and heat capacity.[60–62]

There are apparently anomalous thermodynamic properties in polyamorphic systems; these include excess contributions to thermal expansion, isothermal compressibility and the specific heat capacity. The anomalous contributions to volume in H_2O, based on the differences in macroscopic thermodynamic properties and the non ideal mixing model,[60–62] result in the characteristic density maximum in H_2O. These excess contributions also change with pressure and reflect the increasing stability of the high-density species as the system is compressed. There are also anomalous contributions to the temperature-dependence of heat capacity. Changes in heat capacity as a function of pressure, implied by the increase in the abundance of the high density liquid species indicate that the rheological properties of the liquid will change as a function of pressure. This is a change in the liquid fragility.

Changes in liquid fragility with pressure

The concept of liquid fragility was introduced by Angell,[11,12,22,63] building on earlier work by Uhlmann.[64] Liquid fragility is a measure of departure from Arrhennius Law viscosity–temperature behaviour. A fragility plot (Fig. 5) is produced when the viscosity–temperature relations for different liquids are scaled against the calorimetric glass transitions (T_g). SiO_2 is typically used to define the ''strong'' Arrhennian limit. More ''fragile'' liquids show increasing degrees of curvature in their viscosity when scaled to T_g. Fragile liquids therefore show non-linear increases in viscosity in the supercooled liquid regime. The relationship between the thermodynamic properties of a liquid and the viscosity is considered to be a reflection of the contribution of configurational entropy. This is the basis of the Adam–Gibbs model of viscosity[1] and is seen in the jump in heat capacity (ΔC_P) at the glass transition temperature. A large change in heat capacity corresponds to a fragile liquid and indicates a strong temperature-dependence of liquid structure. The entropy differences between the liquid species in the two-state models should, therefore, correspond to differences in the rheological properties of the liquids. Liquids dominated by the high density species will be more fragile. Since the higher density species will be stable at greater pressures then higher pressure liquids will be more fragile and will have increased

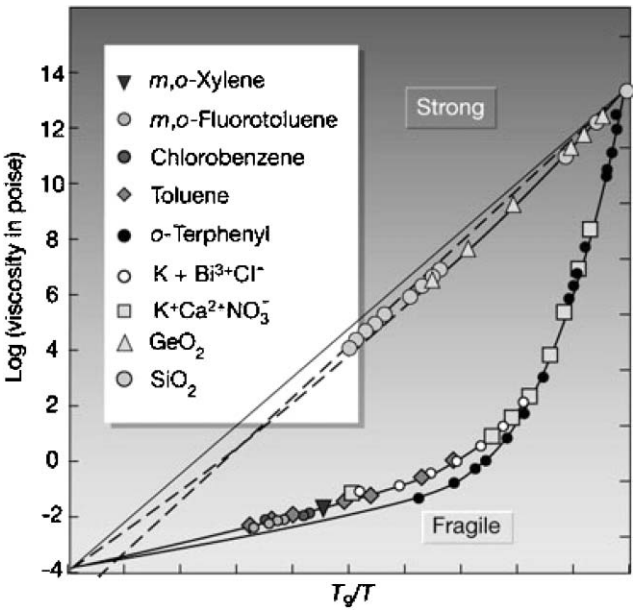

Fig. 5 The liquid fragility. The viscosity and hence relaxation behaviour of several glass forming liquids is plotted as a function of temperature scaled to the glass transition (T_g). Strong network forming liquids have an Arrhenius viscosity–temperature relation while fragile liquids show dramatic changes in viscosity as a function of temperature. The fragility of liquids is also reflected in the jump in heat capacity at the glass transition, *i.e.* the configurational entropy. (Reproduced with permission from Ref. 122. Copyright 2001 Nature Publishing Group.)

configurational entropy. However, the exact structural changes though are unclear and has led to Angell and others[21,65] to develop versions of the two state model that are not based on specific liquid species but on the degree of excitation of the liquid structure (bond-breaking).

In the two state model formulated by Rapaport[30,56] and applied to systems with negative dT_m/dP slopes such as Cs, the two different liquid species have structures that are similar to the high- and low-pressure crystalline polymorphs. Such implied structural changes may be applicable to simple elemental substances but one of the surprising things about systems with reported polyamorphic behaviour is that they are not restricted to simple systems but include systems that are structurally complex such as H_2O,[57,66] BeF_2, triphenylphosphite (TPP),[67–69] GeO_2,[44,45] SiO_2[26,70] and Y_2O_3–Al_2O_3.[71] Structural studies indicate that, for example in the clearly demonstrable case of a liquid–liquid transition in super-cooled Y_2O_3–Al_2O_3,[72–74] the changes in structure are mid- and not short-range (coordination number) order, even though there are difference in short-range order in crystalline polymorphs in these systems. Angell's version of the two-state model emphasises the configurational change and departure from ''ideal configuration'' rather than the presence of specific structural species. Tanaka[75,76] has also used the two-state model as the basis for explaining polyamorphic trends again based on departure from ideal configurations, although in this case the two-state model is based on the competition between density-ordering and bond-ordering (directional, strong covalent bonds). These modified two state models have identical

formulism to the version of Rapaport. Critical-like behaviour and transition between low- and high-density liquids is a reflection of the non-ideal mixing or clustering of the high- and low-density components, referred to as cooperativity.

The bond-ordering model is developed in terms of ''excitation'' from a ground state, but the excitation is not the usual one of electronic origin. The degree of excitation from the ground state is defined as a build up of strain as a function of increased restriction on the packing arrangements of the amorphous structure and is temperature dependent. The bond-excitation takes the form of broken bonds and these bonding rearrangements are cooperative such that the defects, like molecules in classic non-ideal solutions, will cluster. The two-state model of Rapaport[30,56] provides the formalism to calculate a temperature-dependent excitation profile, the state of excitation replacing the fraction of the high-density species. The entropy in excess of the fixed structure (S_{conf}) that results from these configurational excitations can be plotted as a function of temperature (Fig. 6a). The excitation profiles depends strongly on the non-ideal interaction parameter W, that is, the cooperativtity or tendency of the configurational excitations to cluster. At high values of W there is a discontinuity in the excitation profile corresponding to a transition between supercooled liquids that are different in defect content. Such defects are difficult to evaluate in liquid or amorphous states but Angell notes that the same phenomenology can be applied to fluorite-type crystalline lattices. In crystalline PbF_2, a simulation study[21] shows that at low temperatures the population of vacancies and interstitial defects is small but increases dramatically at a critical temperature producing a high temperature (superionic) structure with a liquid-like conductivity. In related compounds the transition is first order and the identified defects are observed to cluster.

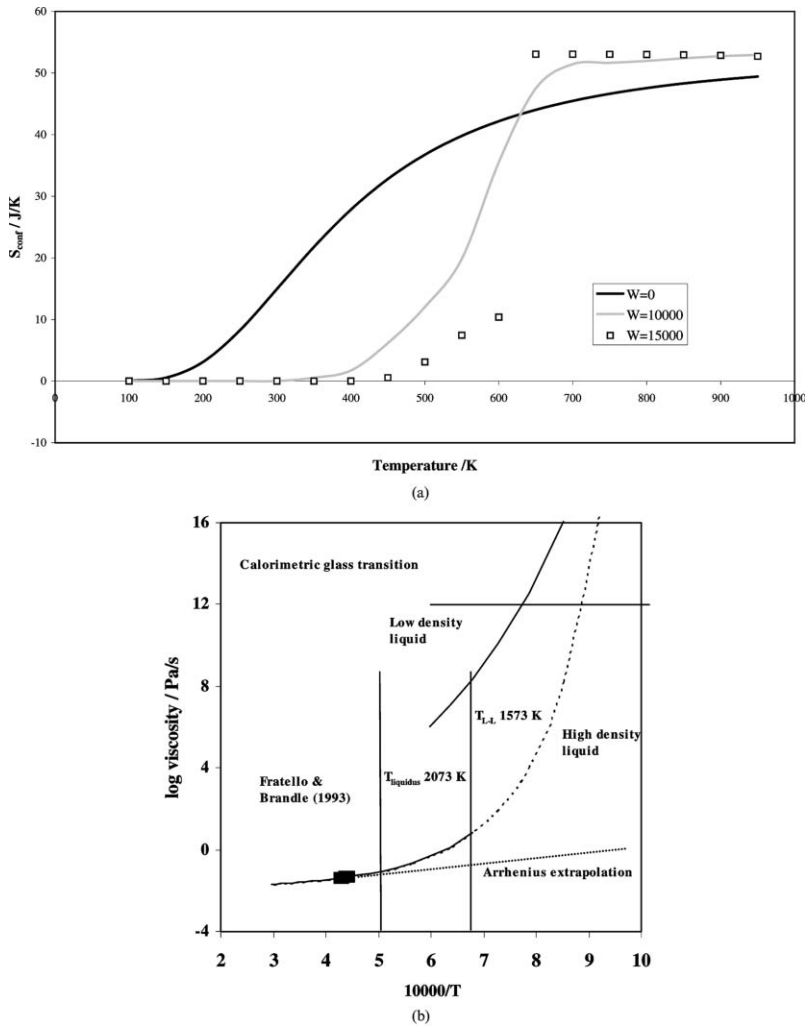

Fig. 6 a. The changing configurational entropy for a simple two-state model using bond-excitation phenomenology.[21] The non-ideal mixing parameter (W J mol^{-1}) determines the steepness of the excitation profile. In the ideal case ($W = 0$) the change in configurational entropy is smooth and the liquid is fragile. With increased W the configurational profile becomes steeper and eventually discontinuous. The discontinuous change would result in a discontinuous change in liquid rheology (fragility). b. The viscosity of the two liquid forms of Y_2O_3–Al_2O_3 close to the composition of YAG ($Y_3Al_5O_{12}$). The stable high density liquid (HDL) is fragile and the viscosity temperature plot can be calculated based on existing high temperature concentric cylinder viscosity data and the calorimetric glass transition. Differences in the relaxation behaviour of the glass formed from the low-density liquid and other calorimetry data[101] can be used to establish the viscosity curve of the LDL. Note the jump in viscosity at the LDL–HDL transition.

The Adam–Gibbs equation for structural relaxation time, an equation that provides a formal link between the temperature-dependence of liquid structure and its viscosity, can be used to determine the fragility of liquids with varying degrees of excitation. The relaxation time τ is written as a function of a term including the activation energy (C), a constant related to the vibrational frequency of the amorphous network (τ_0) and the configurational entropy S_{conf}.

$$\tau = \tau_0 \exp\left(\frac{C}{TS_{conf}}\right) \quad (6)$$

The excess entropy is used to demonstrate the changes in liquid fragility as a function of cooperativity. The transport properties, viscosity and diffusion show increasingly non-Arrhenius behaviour as the degree of cooperativity increases. Ultimately, where there is a suggested phase transition, there is a discontinuity in the liquid rheology corresponding to a fragile to strong liquid transition in the supercooled liquid regime. This is demonstrated for the candidate polyamorphic system Y_2O_3–Al_2O_3 (Fig. 6b). Angell has noted that systems that favour open tetrahedral network structures such as SiO_2, BeF_2, H_2O and Si[63,77] can show sufficiently anomalous behaviour in their fragility (as determined *via* computer simulation) to indicate potential for polyamorphic transition. These tetrahedral liquids may all be considered as candidates for cooperative bond-excitation.

In the version of the two-state model by Tanaka[75,76] the role of strong tetrahedral bonding is further underscored. Tanaka draws a distinction between a view of the liquid state driven by density ordering and a local orientational order. This is based on observations that even in simple liquids spherical molecules favour tetrahedral configurations. Liquids demonstrating the formation of dominant local tetrahedral networks due to strong covalent or hydrogen bonding include SiO_2, H_2O and glycerol. Such liquids have two competing symmetries, one which maximises density and one that maximises the quality of local bonds. Density ordering is consistent with crystalline symmetry but local orientational order is not. Local orientational order can play an important role in stabilizing the supercooled liquid and can result in formation of a glass. The locally favoured structures accompany a decrease in local density; and stability depends on temperature and pressure. The version of the liquid two-state model favoured by Tanaka[75,76] therefore envisages a series of well-defined local structures that are energetically more favourable that normal liquid structures. The proportion of these local structures depends on pressure and temperature and there is the possibility of cooperative effects that can lead to gas–liquid like critical behaviour. In this version, Tanaka uses the concept of local orientational order to explain vitrification, the appearance of critical-like fluctuations in supercooled liquids and also phase separation of supercooled liquids (liquid–liquid transition). Crystallisation requires the destruction of locally-favoured structures because their symmetry is not compatible with crystalline symmetry, this means that there are energetic barriers that have to be overcome in order to form crystalline nuclei, if the liquid is cooling then kinetics may prevent these barriers being overcome and this supercooled state stabilised. Critical-like behaviour can be accessed if the liquid is cooled sufficiently and crystallisation avoided and anomalous light scattering or similar phenomena observed reflecting the instability in bond fluctuations.

Although these two versions of the two-state liquid models are very simplified and are based on the differences in macroscopic thermodynamic properties of amorphous forms of the same substance and phase equilibria, they serve to indicate some of the expected behaviour that may occur if polyamorphism is encountered. Specific, crystal-like clusters are avoided and the models require cooperative rearrangement of amorphous networks. The stability of amorphous networks is strongly dependent on temperature and pressure. Increasing pressure will favour increased density and density-ordering and so liquid fragility and cooperative clustering; possibly leading to liquid–liquid transition may be expected at moderate pressure.

Candidate polyamorphic systems

The two-state models, while avoiding the exact mechanism, do predict certain type of behaviour. These behaviours should be observed in candidate polyamorphic systems. To summarise, candidate polyamorphic systems will have some or all of the following properties; overturn of the melting curve or a negative dT_m/dP slope, non-ideal mixing such that these slopes are no described simple by the ideal mixing of two "species" of different volume (coperativity), pressure-induced amorphisation, a variety of structural motifs in the amorphous or liquid state, different amorphous forms produced by different synthesis routes with measurable thermodynamic differences between them, changes in macroscopic properties such as viscosity and electrical conductivity with pressure and rich phase diagrams with numerous crystalline polymorphs. We will now review some of the classic candidate polyamorphic systems and summarise the evidence supporting transitions between amorphous forms and metastable liquid phases as well as discussing some of the more controversial aspects of this type of liquid behaviour.

Amorphous forms of H_2O

As is well-known, ice will float on water over a range of temperatures. This is reflected in the phase diagram of water where the increase in density on melting is seen as a negative dT_m/dP slope to the melting curve of ice Ih. Liquid water has a maximum in its density at 277 K (4 °C) at atmospheric pressure. When ice Ih is compressed at low temperature, it was found by Mishima in 1984[29] that an amorphous form was recovered. This pressure-induced amorphisation occurs when the metastable extension of the ice Ih melting curve is intercepted and results from a mechanical instability in the lattice and collapse to a metastable amorphous form.

Amorphous ice can also be produced by alternative routes. When water vapour is deposited on a cooled plate an amorphous form can be produced which has a glass transition temperature at 130 K. When heated above this glass transition temperature a high viscosity supercooled liquid is produced. Amorphous ice produced in this way is referred to as low density amorphous ice (LDA) and differs in density from the high density form (HDA) produced by pressure-induced

amorphisation by 20%.[29,57,58] When heated, samples of recovered HDA will transform to lower density LDA. Similarly, when LDA is compressed at 177 K it will transform to HDA over a narrow interval in pressure. Transformation to HDA occurs at 3.2 kbar on compression and HDA transforms back to LDA at 0.5 kbar.[57,66,78] Differential scanning calorimetry experiments on HDA at atmospheric pressure[58] show a glass transition and in the relaxed, supercooled regime an exothermic signature of a transition to the more stable LDA phase. These data are used in two-state models in combination with volumetric data from the phase diagram to indicate the presence of a second critical point and stable liquid structures that resemble the low and high pressure amorphous forms, *i.e.* HDL and LDL.

The structure of liquid water has been extensively studied by both neutron and X-ray diffraction.[79,80] At room pressure and temperature water has been shown to have a network-like structure, with each hydrogen atom coordinated by four oxygen atoms.[81] It is therefore one of the tetrahedral liquids discussed by Angell.[82] Neutron diffraction studies of water at pressures of up to 4 kbar have been performed.[83] For H_2O the total rdf can be considered as comprised of the weighted sum of three partial rdf contributions; $g_{OO}(r)$, $g_{HH}(r)$ and $g_{OH}(r)$. The diffraction data at high pressure show a dramatic change in $g_{OO}(r)$. At ambient pressure $g_{OO}(r)$ has two prominent peaks corresponding to the nearest-neighbour O–O distance (at 2.5 Å) and a second peak at 4.5 Å. As pressure is applied the second peak moves to shorter distances and eventually becomes a shoulder to the first peak. The corresponding changes in both $g_{HH}(r)$, and $g_{OH}(r)$, with pressure are less pronounced. The diffraction data and models of the liquid structure, based on empirical structural refinement,[50,83,84] suggest that, as liquid water is compressed, the open hydrogen-bonded structure collapses to a configuration with non-tetrahedral bond angles. Such a collapse does not prove unequivocally the existence of a liquid–liquid transition but there would be a relationship expected between high pressure forms of water and the HDA form were a two-state or similar model involving a second critical point to be applicable.

The HDA form of ice can be produced in sufficiently large quantities to allow its structure and vibrational properties to be studied. The mechanism of formation, collapse of the ice Ih lattice, would suggest that it may be an amorphous metastable state related to the underlying stable crystal structure, in this case ice XII. As noted by Klug,[85] there are similarities in the $g_{OO}(r)$ of HDA and ice XII. Vibrational properties determined by Raman Spectroscopy and inelastic neutron spectroscopy are strong functions of O–H bond length and provide further insight into the nature of the amorphous HDA form. HDA ice has an excess in the vibrational density states. Infrared and incoherent inelastic neutron scattering techniques and lattice dynamics suggests and origin of this excess in low frequency vibrational modes from several sources including damped acoustic modes, interacting soft harmonic oscillators and quasi localised vibrations. This excess in the vibrational density of states is absent in LDA. These low frequency modes are the origin of the excess in entropy responsible for the increased fragility, *i.e.* the HDA amorphous form is consistent with a more fragile glass-forming liquid.

A comparative study of LDA and HDA, using neutron diffraction with isotopic substitution and combined with empirical potential structural refinement (EPSR)[86] has been used to ascertain the differences in the pair-distribution function of the two forms. Both forms of amorphous ice are fully hydrogen-bonded tetrahedral networks. The structure of HDA resembles that of liquid water at high pressure[87] while LDA is similar to ice Ih.[80] The pair distribution functions for the two forms differ most notably because of the presence of an interstitial water molecule in the HDA form, which lies just beyond the first O–O coordination shell. The presence of this molecule results in HDA being less ordered than LDA. The diffraction data and resulting pair-correlation functions show limited change in the O–H and H–H partial contributions, with a sharpening of the main peaks as LDA is transformed to the HDA form. In contrast there are distinct changes in the $g_{OO}(r)$. The O–O coordination number for the LDA form is 3.7 comparable to the value for low pressure water (4.3). In the HDA form the O–O coordination number is increased to 5.0 and suggests an additional water molecule present in the first neighbour shell. Spatial density functions, obtained from EPSR models of the diffraction data suggest that, on compression, the second neighbour shell of water molecules collapses and water molecules can become interstitial. Finney and others[88] suggest that $g_{OO}(r)$ for the HDA form resembles that of water, but that $g_{OO}(r)$ for LDA and ice Ih have sharper second neighbour O–O peaks. The HDA data cannot be fitted to a crystalline model realistically. The role of interstitial water molecules is apparently to secure the HDA structure and allows this form to be recovered. Interstitial molecules increase in abundance as water is compressed and, in this regard, the HDA form of ice may be regarded as being related to the high pressure form of liquid water. The potential relationship between liquid and amorphous forms is however further complicated by the report of an additional amorphous form of ice.

When the LDA form of ice is compressed to form HDA at 77 K, an additional form can be produced and recovered by isobarically heating the HDA to 140 K. This form has a higher density and is termed very high density amorphous ice (VHDA).[88,89] Diffraction data for VHDA show significant differences in the $g_{OO}(r)$ when compared to that of HDA and LDA. The most obvious changes are increasing intensity in the second neighbour O–O region between 3.1 and 3.4 Å, this is a minimum in $g_{OO}(r)$ for HDA. In the VHDA form, there is a peak that appears as a shoulder to the first O–O peak. This is distinct from the second neighbour peak in HDA which occurs at a greater radial distance and is separated by a minimum between 3.1 and 3.4 Å, indicative of more directional bonding. The VHDA form may, therefore, be viewed as having more disorder in the second neighbour shell. Both HDA and VHDA forms have interstitial molecules which act as, in Finney's terms, a lynch pin securing the amorphous structure and inhibiting relaxation back to an LDA form. It is postulated that VHDA is more representative of the high pressure liquid and has more interstitial molecules present. What it is not clear is how the HDA and VHDA forms are related and whether there is a sharp transition between them. Some authors[90,91] suggest that the VHDA form is more stable form and that

HDA is an intermediate phase. If this was the case then any two-state or similar model would have a second critical point that should be based on the thermodynamic differences between the LDA and VHDA forms.

The change in structure during the transformation between HDA and LDA forms of ice has been studied *in situ* by neutron diffraction with isotopic substitution. Far from clarifying the nature of this polyamorphic change, however, different studies suggest two alternative transition mechanisms; continuous and discontinuous. In a study by Klotz and others[92] diffraction data show a shift in the position of the principal peak in the structure factor as samples are compressed from 0 to 0.7 GPa and on to 2.2 GPa. The Fourier transform of these data show changes in $g_{OO}(r)$ with the second neighbour peak moving to shorter radial distance. The highest pressure data resembles that of the VHDA form confirming the close relationship between the two forms and indicating that the mechanism of formation of the high density amorphous forms is the collapse of the second neighbour shell and formation of an interpenetrating network of water molecules. The three diffraction data sets indicate three different structures and a potential transition from LDA to VHDA by an intermediate HDA form.[92]

The presence of intermediate forms of amorphous ice has been suggested by Tulk and others.[93] In the region of transition, diffraction studies using both neutrons and high energy X-rays show changes in the position and shape of the first peak in the diffraction pattern (Fig. 5). In addition the relaxation to these intermediate amorphous forms has been monitored by annealing HDA at different temperatures. The formation of intermediate structures over the completed transition from HDA to LDA has been shown by Guthrie and others.[4,94] The change from HDA to LDA represents a shift in the first peak in the structure factor from 2.1 to 1.7 $Å^{-1}$ and there are similar dramatic changes in the real space transform of these data, *i.e.* the $g_{OO}(r)$ (Fig. 7). The changes in O–O correlation in the 2.75 to 4.5 Å range are seen as the depletion of the interstitial oxygen in the 3.6 Å region. This is seen as the shoulder to the first O–O peak becoming more distinct and moving to a greater radial distance through the transition from HDA to LDA.

A study of the transition from LDA to HDA at 130 K and 0.3 GPa has, by contrast, been interpreted as a first order transition.[95] The neutron data in this study has been interpreted as a linear combination of the HDA and LDA components. This study suggests the nucleation and growth of the HDA phase in a matrix of the LDA assuming crystal-like behavior and using an arbitrary shift parameter to model the shift in the first diffraction peak. This does not account for the dramatic changes in intermediate-range order demonstrated by Guthrie and others[94] (Fig. 7).

The current debate on LDA–HDA transition focuses mainly on the presence of the second critical point that is suggested by two-state and similar models. The data of Tulk, Guthrie and others argues against its presence since the transition is continuous. From versions of the two-state models currently favoured by Angell, Tanaka and others,[21,75] however, a second critical point does not have to be present, the liquid or supercooled liquid needs only to show strong cooperativity. If

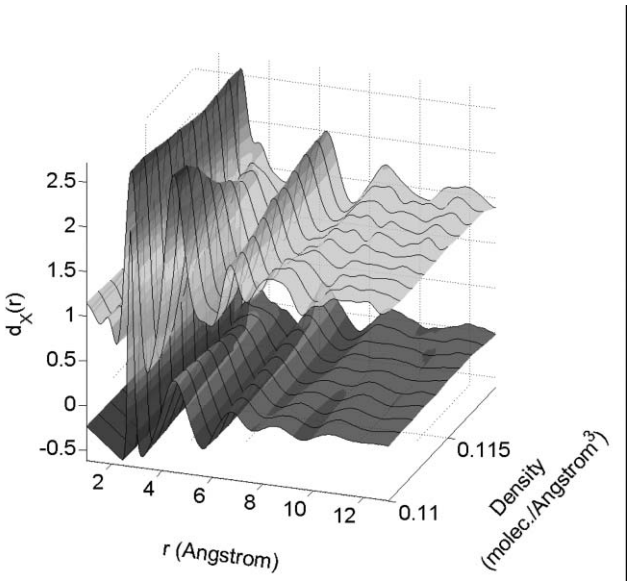

Fig. 7 Oxygen–oxygen partial differential distribution function for amorphous ice.[4] The diffraction data (X-ray) is shown at the top while the results from a molecular dynamics simulation are shown at the bottom. The collapse of the second shell (at around 3.6 Å) can be clearly observed as the density increases and the interstitial molecules are pushed into the first O–O shell.

the non-ideal mixing parameter (W) in the bond-excitation version of the two-state model is zero then configurational entropy changes with temperature will be smooth and continuous and a fragile liquid will result provided that the entropy change associated with bond-breaking is high. If W is non-zero the configurational entropy profile becomes increasingly steep, but continuous. It is possible to produce profiles for large values of W where the values of configurational entropy will change rapidly over a narrow temperature region but without the need for a discontinuous, first-order transition or a second critical point (Fig. 4b). These intermediate states would have different relaxational properties and fragilities but would be highly cooperative systems. Without recourse to complicated interpretations it can be seen that the behavior of amorphous forms of ice can be interpreted in these terms.

Amorphous silicon

Crystalline silicon has a semi-conducting tetrahedrally-coordinated diamond-structured polymorph that is stable at low pressure. At high pressure the tetrahedral structure collapses and a metallic phase with octahedral coordination of silicon is stable, the β-Sn phase.[54,96] The melting curve of the low pressure polymorph has a negative dT_m/dP slope which indicates an increase in liquid density on melting and suggests that silicon might be a candidate polyamorphic system. Amorphous forms of silicon can be made at atmospheric pressure by chemical vapour deposition and similar synthesis techniques. The amorphous forms are semi-conducting and have a tetrahedral structure, while the liquid at atmospheric pressure is metallic. The low pressure amorphous forms are not, therefore, quenched representatives of the low pressure liquid and may suggest that there is more than one form of

amorphous silicon and a possible transition between different phases.

At high pressures the liquids have a coordination number greater than four, and this liquid cannot normally be quenched to a glass. One consequence of the negative dT_m/dP slope is the potential for pressure-induced amorphisation. When porous nanophase diamond-structure silicon (π) is compressed an amorphous phase can be produced. In the demonstration of pressure-induced amorphisation, Raman spectra and X-ray diffraction data were collected as π-silicon was compressed in a DAC.[96] The diamond structure is shown by a strong (111) reflection which is present up to pressures of 7–8 Gpa. The structure is completely amorphous at 12 GPa. Raman spectra collected simultaneously show a red luminescence that shifts to increasingly longer wavelengths with pressure. At high pressures, coincident with the amorphisation of the sample, this band disappears and is replaced by a weak broad feature between 200 and 400 cm^{-1}. The high pressure Raman spectrum is different from that of amorphous phases produced at ambient pressure but does resemble that of β-Sn. As a result the high density amorphous form of Si is tentatively assigned an HDA form.

On decompression the Raman spectrum of the amorphous form changes. The HDA Raman signal persists until 10 GPa at which point a broad amorphous band at 470 cm^{-1} appears, a signal characteristic of the low pressure amorphous form *i.e.* an LDA form.

Based on the available thermodynamic and computer simulation data,[54,97] a two-state model can be constructed for Si. This predicts an amorphous–amorphous transition in the pressure range where the Raman signal changes. An interesting feature of this simple model is that the position of the second critical point occurs at a negative pressure (under tension) and means that if the liquid stable at atmospheric pressure is supercooled then it will intercept a liquid–liquid transition in the supercooled regime and an LDA form would result different in structure and electronic properties from the low pressure liquid.

As noted from the Raman study, the optical properties of the amorphous forms of silicon change on compression. At high pressure the reflectivity of the HDA form is greater than the metallic gaskets used in the diamond anvil cell and suggests that the HDA form is metallic. Electrical resistance measurements also change dramatically in the vicinity of the proposed HDA–LDA transition.[54,97] The two-state model predicts a transformation between LDL and HDL supercooled liquids at approximately 1060 K. This temperature is coincident with the ''unusual'' melting transition reported when amorphous (LD) silicon is heated to the crystalline melting temperature. Molecular dynamic simulations using the Stillinger–Weber potential[98] have been used to explore this region in temperature. Above the proposed LDL–HDL transition region, the equilibrated volumes in the simulation show fluctuations consistent with thermal fluctuations. Closer to the transition however, the fluctuations in volume are much greater and the magnitude consistent with the density differences between the LDL and HDL liquids. There are changes in mean coordination number associated with these fluctuations, the higher density fluctuations showing a greater proportion of 5- and-6

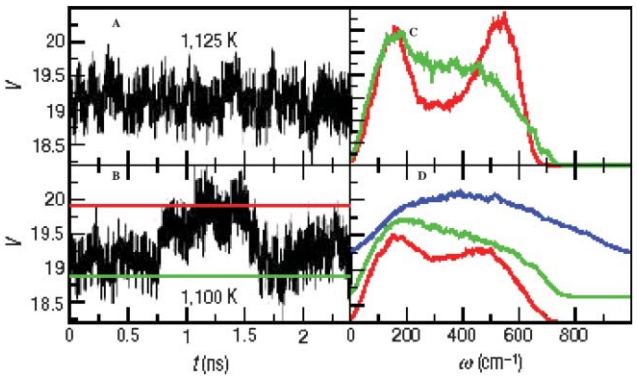

Fig. 8 Results of molecular dynamics simulations of supercooled liquid silicon. Constant pressure runs carried out at 1125 K and 1100 K show contrasting fluctuations in volume. At 1125 K the equilibrated volumes show normal fluctuations (A) as a function of time (in nanoseconds) but as the HDL–LDL transition is approached the system shows large random fluctuations in volume between low (red) and high (green) density configurations (B). The calculated Raman Spectra (C) for the 1100 K simulation fluctuate between a two-peaked structure (LDL) and a single broad maximum (HDL), ω is frequency. When the supercooled LDL (red) liquid is compressed (D), the Raman spectra show a transition from the two-peaked LDL configuration to the single broad peak of HDL at high pressure (blue) consistent with the existence of an LDL–HDL transition.

coordinated silicon. These simulations suggest critical-like fluctuations in the supercooled regime (Fig. 8). The vibrational properties calculated from the simulations show distinct low- and high-frequency peaks associated with stretching and bending of tetrahedral silicon in the LDA network. The HDA spectrum has a broad feature associated with an increase in 5- and 6-fold domains and is consistent with the increased fragility of the HDL supercooled liquid. This indicates that the behaviour of supercooled liquid silicon is consistent with a strong to fragile liquid transition accompanying the LDL–HDL transition, increased low frequency modes contribute to the increased configurational entropy of the HDL liquid.

Liquid phosphorus

Liquid forms of phosphorus have complicated structures. Metallization in the liquid state has been reported at pressures of between 0.7 and 1.2 GPa, at which point the electrical conductivity is observed to increase.[25,27] Grain size differences in recovered samples are taken to indicate that there are rheology changes in this region too. The crystalline phase diagram for phosphorus is rich. White phosphorus, which has a low melting point (44 °C) is tetrahedral consisting of P_4 molecules. Red phosphorus has a polymeric structure with a correspondingly higher melting point (>600 °C). Black phosphorus has a layered structure and consists of three-coordinated atoms. The melting curve of black phosphorus shows a maximum at 1 GPa. This is the region where electrical conductivity is seen to change and is the point at which the liquid density is greater than that of the crystalline phase.

X-ray diffraction studies of the liquid performed at high pressures between 0.77 and 1.38 GPa show a dramatic and sudden change in structure.[28] At pressures of 0.77 and

0.98 GPa the structure factor shows a prominent first peak at 1.4 $Å^{-1}$. At pressures of 1 GPa this first peak is reduced in intensity and a new maximum is developed at 2.45 $Å^{-1}$. The Fourier transform of these data shows, at low pressures, peak centred on 2.2 Å, corresponding to the P–P distance in P_4 molecules.[25,28,34] The intensities of the next-nearest neighbour P–P peaks are low and the low pressure liquid structure is interpreted as comprising an open tetrahedral framework. At pressures greater than 1 GPa, the P–P peak shifts to a greater radial distance and there is an appearance of pronounced next-nearest peak at 3.5 Å. This peak is interpreted as being characteristic of an increasingly polymeric liquid. The two different liquids have different densities, estimated from the pdfs as 2.0 g cm^{-3} and 2.8 g cm^{-3} for the low and high density liquids respectively.

Following the initial observation, subsequent X-ray diffraction studies have concentrated on characterizing the changes in liquid structure at higher temperatures,[99] effectively mapping the suggested LDL–HDL transition curve as a function of pressure and temperature. The *in situ* data show that the lowest pressure and highest temperature at which there is a transition between the two liquids occurs at 0.3 GPa and 2200 °C. The transition between the low density molecular form and the high density polymeric form is also seen as changes in the first peak in the diffraction pattern. A similar trend is observed in computer simulations which also predict a change in electrical conductivity.[100] The transition between the two liquids would be expected to terminate in a critical point. What is surprising about liquid phosphorus is that the transition emerges into the stable liquid fields and no critical point or critical-like fluctuations have been reported. Radiography data from Katayama[25,34] clearly demonstrate the nucleation and growth of one liquid in the matrix of another as predicted by two-state and similar models. The occurrence in the stable liquid field is unusual but can be thought of as consistent with Tanaka's two-state model,[75] that is, if a system shows strong directional bonding that acts in competition with density-driven ordering then the melting temperature based on density-ordering (close packing) may be much higher than the experimental melting curve. If this situation were applicable to liquid phosphorus then the LDL–HDL transition is in effect in the regime below the density ordered melting curve because of the strong directional bonds. A second critical point in this interpretation could again occur at slightly negative pressure. More recently it has been noted that the transition between the LDL and HDL forms of liquid phosphorus occurs above the critical point for the white form of P, which melts at 44 °C;[99] *i.e.*, the "liquid" produced in the decompression experiments is a molecular tetrahedral fluid and the transition is actually between LDL and polymeric HDL fluid phases.

Y_2O_3–Al_2O_3 liquids

Y_2O_3–Al_2O_3 liquids, with compositions close to that of YAG ($Y_3Al_5O_{12}$ garnet) provide a type example of a polyamorphic system, in which a density-driven liquid–liquid phase transition was observed to occur directly.[71] In some respects, however, Y_2O_3–Al_2O_3 liquids provide unusual candidates for polyamorphism. The liquids are structurally complex and have a range of coordination environments around the metal and oxygen atoms. When supercooled Y_2O_3–Al_2O_3 liquids will nucleate and grow a second liquid phase and both liquids can be quenched to glasses that are compositionally identical but with different thermal and mechanical properties (Fig. 9a). Because the transition from the stable HDL to a supercooled LDL in Y_2O_3–Al_2O_3 occurs at room pressure sufficient quantities of glass can be produced of both amorphous forms for diffraction and calorimetric studies.

The HDL and equivalent glass (HDA) is characteristic of a fragile glass forming liquid. When single phase HDA is heated through the glass transition in a Differential Scanning Calorimeter (DSC) an exothermic signature is seen in the supercooled regime that is interpreted as the transition from

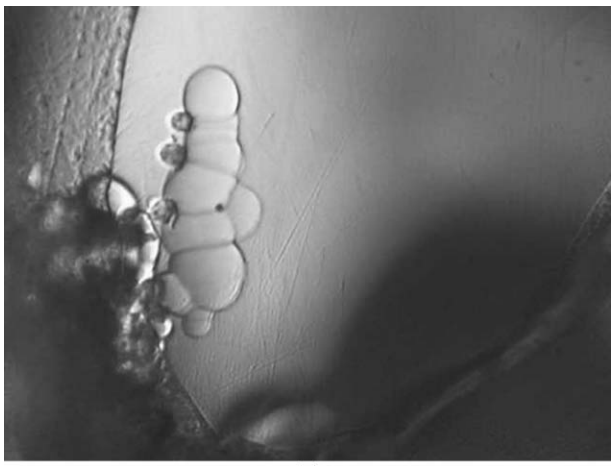

(a)

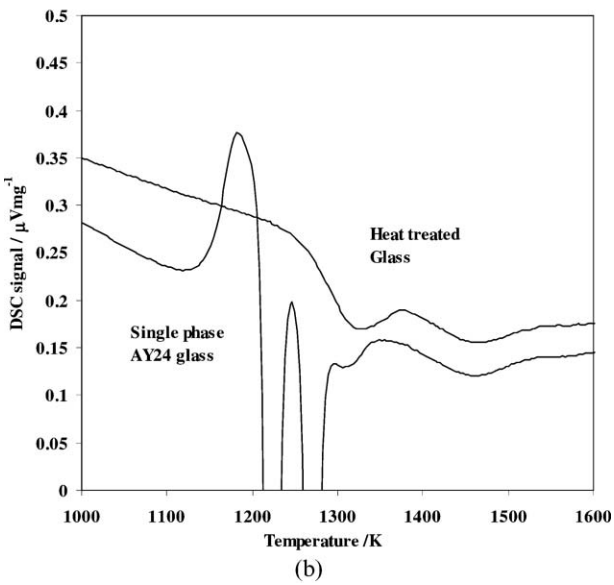

(b)

Fig. 9 a. Plane polarised light image of the two amorphous forms of Y_2O_3–Al_2O_3 glass quenched from the supercooled liquid regime. b. Differential scanning calorimetry (DSC) signal for a single phase glass (HDA) quenched from a 24% Y_2O_3–76% Al_2O_3 liquid. The glass transition for the HDL liquid is identified and followed by two exothermic peaks, one of which (1275 K) is the transition between the supercooled HDL and a LDA glass. When the sample is reheated the HDL glass transition is absent and the LDL glass transition (at 1300 K) is the only exothermic feature present.

supercooled HDL to a more stable LDA form. Crystallisation also occurs in this region but is kinetically inhibited. This exothermic signature is similar to that reported by Whalley and others[58] when HDA ice is heated above its glass transition. The LDA form of Y_2O_3–Al_2O_3 has a glass transition temperature at a higher temperature and shows characteristic features of a strong liquid. Calorimetry[101] studies have established the entropy differences between different amorphous forms and a two-state model can be used to confirm the location of the LDL–HDL transition on the basis of these data (Fig. 9b).

Neutron and X-ray diffraction studies of single and composite Y_2O_3–Al_2O_3 glass samples have been carried out.[74,102] These data show that there is little change in the short-range order on transition, coordination numbers of Al–O and Y–O remaining unchanged as the LDL–HDL transition is crossed. There are, however, changes in the mid-range (metal–metal correlation) order. The neutron and X-ray data sets can be combined to eliminate specific partial structure factors and to identify the structural contribution of the LDA form to the total diffraction pattern. Eliminating the O–O correlations from the total pair-correlation function helps clarify the positions of the yttrium–yttrium, yttrium–aluminium and yttrium–aluminium correlations (Fig. 10). The single phase HDA samples have peaks at 3.25 and 3.62 Å in the total pdfs. The Al–Al correlation contributes primarily to the peak at 3.25 Å, while the Y–Y and Y–Al distances are reflected in the peak at 3.62 Å. The total X-ray pdf for the two phase LDA–HDA glass does not correspond to the same distribution of Y–Y, Y–Al and Al–Al distances. The results from Reverse Monte Carlo fits to diffraction data and polarizable ion molecular dynamics (PIMD) simulations on the same base compositions[72,103] provide important insight into the short and mid-range order changes in Y_2O_3–Al_2O_3 aluminate liquids. The main structural differences and the mechanism for the polyamorphic transition are seen in changes in connectivity and arrangement of the Al–O and Y–O polyhedra that form the glass structure. The characteristic distances, Al–Al, Y–Al and Y–Y, for different polyhedral arrangements can be used to estimate the relative proportions of different polyhedral configurations. For the single phase high-density Y–Al glass sample the two peak at 3.25 and 3.62 Å reflect 70% of the Y–O polyhedra occur within edge-shared environments, whereas ~70% of the AlO_4 tetrahedra engage in corner-sharing with the Y–O units. The total pdf derived from X-ray studies of the two phase glass, does not give rise to the same distribution of polyhedra and it appears that there is an increased contribution from edge-shared Y–O and Al–O polyhedra in the LDA form. The proposed structural configurations are shown in Fig. 10.

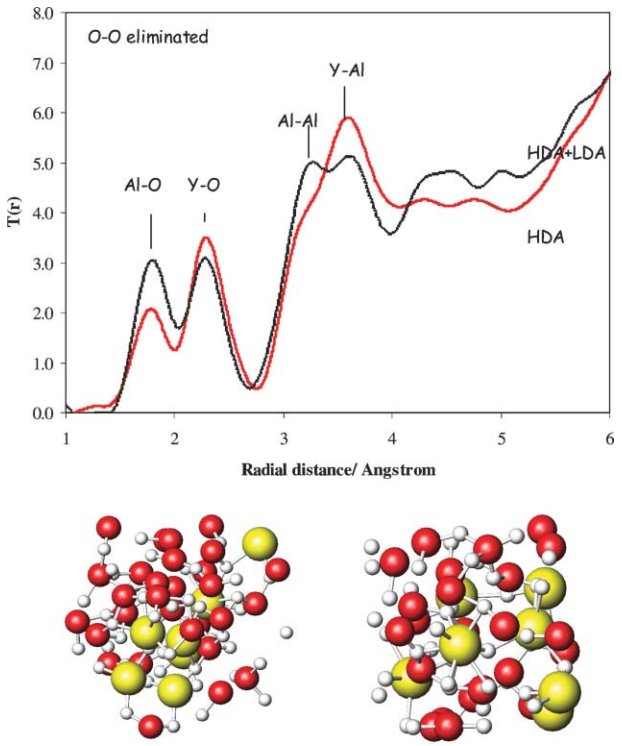

Fig. 10 Total pair correlation function for HD and LD glasses quenched from Y_2O_3–Al_2O_3 liquids. This data is the Fourier transform of a weighted difference $S(Q)$ using both neutron and high-energy X-ray diffraction data. The differences in the Al–O and Y–O peaks reflect differences in composition but the main changes seen on transition are the changes in Y–Al and Y–Y correlations, the intermediate range order and an inferred clustering of Y–O polyhedra in the HD-form. Removal of the HDA contribution to the composite diffraction pattern and reverse Monte Carlo (RMC) modelling provides two possible configurations for the HD- and LD amorphous forms.

Transitions in the strong amorphous networks GeO_2

GeO_2 and SiO_2 are classic network-forming glasses with corner-shared tetrahedral networks and "strong" behaviour. GeO_2 glasses, when compressed, are believed to show an amorphous–amorphous transition from a glass with an open network structure based on corner-linked tetrahedra, at low pressure, to a glass structure dominated by GeO_6 octahedral units at higher pressure. This conclusion is based on XAS measurements that show a change in Ge–O distance consistent with the analogous tetrahedral–octahedral change in crystal phases and Raman spectroscopy data using a diamond anvil cell. *In situ* neutron diffraction studies of GeO_2 (combined with high energy X-ray diffraction studies and molecular dynamics simulations) have been used to investigate the nature of the change in short- and intermediate-range order[44,104] It has also been suggested that vitreous GeO_2 may undergo a first order amorphous–amorphous transition.[15] As GeO_2 glass is compressed the height and position of the first peak in the structure factor changes and indicating a decrease in intermediate range order[44,104] through the shrinkage and collapse of the open network structures (Fig. 11). Prior to a coordination change there are changes in the O–O correlations as oxygen atoms move closer to central germanium atoms. Between 6 and 10 GPa the nearest neighbor coordination number increases and a mixture of 4, 5 and 6 coordinate germanium-centered polyhedra co-exist. This is again an intermediate state and not simply a mixture of 4 and 6 coordinate Ge. As the pressure is increased to above 15 GPa a high pressure octahedral glass forms, which is not recoverable. This network comprises of a mixture of edge- and face-shared GeO_6 octahedral units.

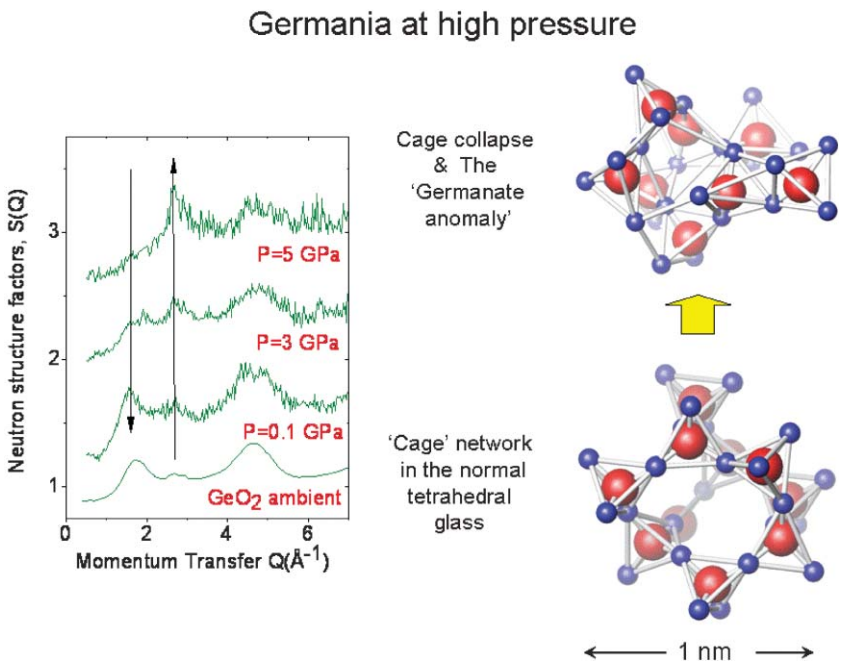

Fig. 11 The measured neutron diffraction signal from germania at high pressure showing the disappearance of the FSDP (collapse of cages in the network) and rise of the second connectivity peak just prior to the start of formation of GeO_5 units at 6 GPa.[44,104]

Non-oxide glasses: $GeSe_2$

Network glasses of AX_2 stoichiometry exhibit a variety of structures, depending on constituent atoms and the character of bonding. Short-range order is reflected in well-defined structural units such as AX_4 tetrahedra, which are linked to form networks and rings with varying members.[6,47,105] $GeSe_2$ is considered an archetypal network-forming glass.[47,105,106] Unlike AX_2 oxides glasses such as GeO_2 and SiO_2, however, $GeSe_2$ has a considerable number of homo-nuclear bonds and consequently, there are a greater variety of different packing arrangements that can be made in response to changes in pressure. This is reflected in the amplitude of the first sharp diffraction peak (FSDP) in the diffraction pattern.[4,107]

The structure of $GeSe_2$ has been extensively studies by neutron diffraction with isotopic substitution[107] and by *ab initio* computer simulation.[108] The basic structural unit is the $Ge(Se_{1/2})_4$ tetrahedron and the diffraction data imply a large number of different arrangements of these polyhedra. The ambient pressure glass structure comprises both edge- and corner-shared tetrahedral arranged in a open framework with a non-uniform arrangement of Ge and Se atoms in which chemical order is broken by homo-nuclear (homopolar) bonds.

The structure of $GeSe_2$ liquids has been shown to change as a function of both temperature and pressure.[109,110] *In situ* studies of liquid $GeSe_2$ under pressure[109] show changes in the intermediate range order as evidenced by changes in the FSDP and these are interpreted as a change from a two-dimensional network to three dimensional fluid. This has led to the suggestion that $GeSe_2$ may show a first-order liquid–liquid transition under the application of pressure. There are additional characteristics of the $GeSe_2$ system that suggest polyamorphism. There is an increase in density on melting indicating a negative dT/dP slope to the melting curve and the different amorphous structures that can be produced mimic the structures of crystal polymorphs. In addition there are changes in electrical properties as the pressure is increased. The low pressure semi-conducting form transforms to a metallic amorphous form at 9 GPa. Recent *in situ* studies of amorphous $GeSe_2$ using high energy X-rays and a diamond anvil cell[111] show changes in structure as samples are compressed. These changes are seen as a decrease in the intensity of the first sharp diffraction peak, which also shifts in position from 1.01 to 1.23 Å^{-1} and an increase (by a factor of 1.46) in the intensity of the principal peak in the X-ray $S(Q)$. The response to pressure, an increase in density, is accomplished by changes in both intermediate- and short-range order. The changes in $GeSe_2$ are qualitatively similar to those in GeO_2. For $GeSe_2$ the changes in intermediate range order are a conversion from edge- to corner-shared $Ge(Se_{1/2})_4$ tetrahedra up to pressures of 3 GPa. Above 3 GPa the response to pressure is an increase in coordination number from a mean Ge coordination number of 3.98 at ambient pressure, increasing from 4.15 to 4.52 between 3.9 and 9.3 GPa. The mechanisms differ in detail between GeO_2 and $GeSe_2$, with the intermediate range order changes in GeO_2 reflecting the greater ionicity in the oxide glass. Tetrahedral GeO_4 units can only be corner shared and intermediate order changes reflect a decrease in void space which becomes accompanied by short-range changes increasing the coordination number from 4 to 5 through intermediate 5-coordinate polyhedra.[111] In $GeSe_2$, because of the homo-nuclear bonding the connections between structural units is very different and density can increase by a change from edge- to corner-shared tetrahedral units. The *in situ* study is consistent with Raman spectroscopy data[112] where the ratio of edge- to corner-shared tetrahedral

units reduces from 34% at ambient pressure to 20% at 3 GPa.[113] This change is apparently continuous and the reported disappearance of the FSDP does not correlate with an amorphous–amorphous transition. Densification apparently occurs by stabilizing a series of intermediate structures and does not occur over a narrow pressure range, although in the relaxed liquid the change in structure occurs between 4.1 and 5.1 GPa.[114] It has been further suggested[4] that the changes in intermediate range order are similar for other tetrahedral systems (Fig. 2). A comparison of the peaks in the structure factor and mean inter-atomic spacing as a function of pressure show similar trends towards a limit, which is the dense packing of random spheres. This would favour an increase in disorder as pressure increases.

Tri-phenyl phosphite (TPP)

A surprising candidate for polyamorphic transition is the aromatic fragile glass-forming liquid tri-phenyl phosphate, $P(OC_6H_5)_3$ or TPP.[67,69,115] The structure of this liquid is more complicated than the elemental or more conventional glass forming systems described above. When TPP is cooled below its melting point at 295 K it forms a glass at a transition temperature of $\sim$205 K. This amorphous state has all the characteristics associated with fragile glass-formers. If the supercooled liquid is, however, annealed at temperatures of 210 to 223 K a new, apparently amorphous, form is observed to nucleate and grow. This amorphous form of TPP is termed the ''glacial phase'' and while it is generally accepted that there are now Bragg peaks, its structure is debatable. The glass phase is described as being nanophase, defect ordered or mixtures of nano- and micro-crystallites. However some authors believe that the glacial form is an LDL-liquid that nucleates and grows in the matrix of the supercooled HDL fragile liquid.[67] Recent studies have demonstrated distinct calorimetric signatures for the transition between HDL and LDL in TPP.[116,117] Furthermore Tanaka and others have demonstrated visually the nucleation and growth of the LDL (glacial) form in a matrix of HDL TPP when supercooled.[75] This is similar to the textures produced when Y_2O_3–Al_2O_3 liquids are supercooled. Furthermore, the calorimetric study of TPP yields data that is qualitatively similar to that of both YAG and HDA ice.[116,117] When the HDL glass of TPP (HDA) is heated to its glass transition and into the supercooled relaxed fluid an exothermic signature is apparent at 225 K whilst, at a temperature of 240 K, the sample crystallizes and, between 225 and 240 K, the sample is identified as the glacial form. Overall, therefore, there is a transition from supercooled HDL to a more stable LDA form, avoiding crystallization (which is kinetically inhibited). The glass transition of the glacial form occurs at 220 K and is much broader than that of the HDA form of TPP. This is consistent with a decrease in fragility (the relaxation time changes less rapidly with temperature in stronger liquids and the glass transition temperature would be higher).[116] When the LDA glass transition is crossed TPP will crystallize from the supercooled LDL at 240 K. Small angle scattering data in the vicinity of the LDL–HDL transition show an increase in small angle signal and this is taken as an indication that the glacial phase is a poorly crystallized phase with an unusually large unit cell, this SAXS data could however also reflect critical like fluctuations (on an 80 Å) scale characteristic of the nucleation and growth of the LDL phase.[118]

Mechanisms for polyamorphism

In the examples given above, there has only been limited discussion of the interactions on an atomic scale that are responsible for the polyamorphic behaviour. Most discussion has been restricted to the structural signatures and bulk thermodynamic properties that are used to construct two-state or similar models. Trends that are seen in polyamorphic systems follow those identified by Angell.[82] These are, that candidate liquids are tetrahedral or characterised by strong directional bonding, and that the transition form one liquid to another involves a change in configurational entropy and consequently liquid fragility.

Many of the candidate systems, such as H_2O and silicon, have been the subject of computer simulation studies. Indeed, many candidates have been identified on the basis of anomalous properties identified in these studies. Much of the discussion of liquid–liquid transitions has been based on the changes that occur in water. Water, as is well known, demonstrates a density maximum at 4 °C. In the supercooled region the extrapolated anomalies in thermal expansion, isothermal compressibility and specific heat capacity all become infinite at −45 °C. Simulations must account for this apparent singularity at −45 °C as well as the presence of the two amorphous forms of ice and equivalent liquids (HDL and LDL).[90]

A first order transition between LDL and HDL was hypothesised based on computer simulation of water using the ST2 potential[119] and a second critical point proposed in the supercooled region. If the LDL–HDL transition line is extrapolated above the critical point the analytical extension can be drawn and this represents a line of apparent singularities. On approach to this singularity thermodynamic properties diverge but ultimately remain infinite. A possible explanation of this type of behaviour is to consider inter-atomic potentials with more than one minimum.

In their crudest form these type of double-well potential describe static heterogeneities in supercooled liquids.[90] There are LDL and HDL configurations. The double well potentials have minima that correspond to these configurations, a deeper LDL minimum with a low entropy and high volume (low density) and a shallower HDL minimum with higher entropy, lower volume. The shifting balances between the two minima will presumably depend on pressure and temperature and the cooling history will ultimately determine which configuration is adopted. Computer simulations that have explored the nature of static heterogeneities using a variety of different potentials have reported fluctuations between heterogeneities of well-defined volume.

One particularly useful form of potential used in this type of simulation is the soft-core potential. These favour two distinct types of particle–particle separation and can result in transitions between the two configurations, *i.e.* transition between liquids of difference density. Core-softened potentials can have

two forms: a shoulder which in which the hard-core regions shows a region of negative curvature or a step and ramp potential in which the hard-core is ''softened'' by a linear slope. Ramp potentials or families of ramp potentials can be used to model the separation of LDL and HDL phases.[120] The potentials, or families of potentials, have a minimum radial distance and depth of well tuned to a constant value of the second virial coefficient. Monte Carlo simulations using these potentials have been used to explore regions of LDL–HDL coexistence and associated thermodynamic anomalies and density maxima.[120] In these studies, it has been found that in the stable LDL field the number of nearest neighbour located at the potential minimum are greater. In the HDL field there are a greater number of neighbours at the hard core distance, even though this is energetically more expensive. As temperatures are lowered through the LDL fields density maxima are encountered, this is where there is the maximum number of neighbours of the hard core distance value (the closest approach). Altering the ramp potential for different values of minimum distance and well depth shifts the location of the LDL–HDL transition to lower temperature and pressures and the transition can be rendered metastable with respect to the hexagonal and cubic-close packed crystalline phases. Density maxima obtained in this way extend into the stable fluid region.

The use of realistic potentials in modelling LDL–HDL transitions is effective shorthand for a description of the so-called energy or configurational landscape. The terminology associated with energy landscapes can be used to describe, conceptually, the onset of polyamorphism. As has been noted by Angell and others,[21,63,82] there is a close link between polyamorphism and liquid fragility, or configurational entropy. Fragile liquids will have a complex energy landscape, that is the potential energy surface will have a large number of configurational minima which can be explored by temperature activated processes. On cooling these configurations can be trapped in local minima and the liquid will become non-ergodic. The final structure will depend on cooling process and the thermally activate process is structural relaxation. This means that the fictive temperature of a glassy phase is a configurational minimum in this energy landscape. Strong liquids in contrast have few minima in their energy landscapes, which are not necessarily those of the crystal (*i.e.* strong directional bonding) and glasses will form more readily. The LDL–HDL transition can be described in configurational landscape terms. The LDL and HDL configurations are viewed as different minima in the potential energy surface, as suggested by PIMD and ramp potential simulation. Under certain conditions (supercooling) configurations can fluctuate between minima as seen in the Si and Y_2O_3–Al_2O_3 simulations. The exact nature of the energy landscape will change with pressure. The gap or barrier between different minima in the energy landscape (termed a density gap) will change as will the depth of minima reflecting the stabilisation under pressure of increased density configurations. Critical behaviour would be the tunnelling through the density gap by first order transition, but continuous changes can be accommodated if intermediate minima become stable under pressure.

Future directions

The structures of chemically complex liquids and glasses can be studied in detail if the partial structure factors can be determined either by neutron and X-ray diffraction techniques. The pair distribution function is the starting point for interpreting amorphous structure and diffraction data used in combination with computer simulation and spectroscopy provide a means for interpreting the short- and intermediate-range structure, reproduced in the $S(Q)$ or $G(r)$, that is characteristic of polyamorphism. Developments in the specialised sample environments for use in combination with neutron diffraction mean that the change in liquid or glass structure with pressure and temperature can now be ascertained. Although few studies on the changes in amorphous structure with pressure have been made, they generally show large changes in both intermediate and short range order. The nature of these changes remains controversial with regard to polyamorphism and the high pressure liquid regime is as yet largely unexplored. As sample environments become developed there are opportunities to probe extremes of temperature and pressure offered by the advent of new neutron and X-ray sources and instruments. The Spallation Neutron Source (SNS) being developed at Oak Ridge national Laboratory (US) and the new second target station at ISIS, Rutherford Laboratory (UK) for example, will offer high neutron fluxes and there is the opportunity to examine small samples such as those contained in high pressure cells. Disordered and isotopically-substituted materials such as $^{11}B_2O_3$ (Fig. 12), can be examined and structural changes determined.

Summary

In conclusion then, density- or entropy-driven liquid–liquid phase transitions occurring at constant composition could be a quite general aspect of liquid and occur in a variety of systems.

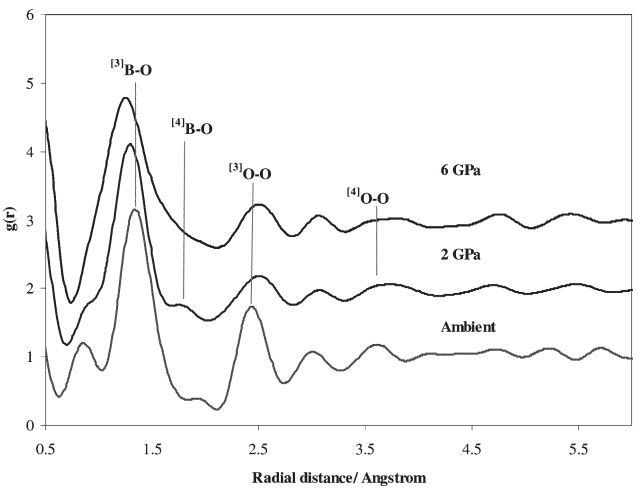

Fig. 12 Preliminary results from an *in situ* neutron diffraction study for $^{11}B_2O_3$. The ambient pressure data shows boron atoms coordinated by three oxygen atoms as pressure is increased the B–O coordination number increases to four, with corresponding shifts in the O–O correlation. There are only three pressure points reported in this experiment. Open questions remain. Do for example the increase in B–O coordination occur smoothly or is the change a discontinuous jump?

In some systems, the behaviour observed constitutes changes in physical properties in the liquid regime rather than a true liquid–liquid phase transition, or occurs in the non-ergodic glassy regime. The existence of such large property changes points to the existence of a density-driven transition at some lower temperature that may be experimentally inaccessible with current techniques. No single criterion is identified as being characteristic of polyamorphic transitions. There are several indications in overall liquid behaviour that make some liquids candidates for LDL–HDL transitions. These include; low pressure liquids dominated by open tetrahedral frameworks or structures with strong directional bonds, maxima in the dT_m/dP curves, including for example $GeSe_2$,[6,47,107] and the possibility of pressure induced amorphisation, increasing liquid fragility with pressure and cooperative behaviour. These would be seen as non ideal behaviour and anomalous thermodynamic properties such as density maxima, changes in electrical properties with pressure and critical-like fluctuations. Structural changes are most likely to involve medium rather than short range order[6,47,107] and transitions between amorphous forms can be continuous.

The existence of such L–L phase transitions driven by density (pressure) and entropy (temperature) differences between the two liquid phases constitutes a new field for exploration in the physical chemistry of the liquid state. For each system in which the phenomenon is described, a major challenge will be understanding the differences in liquid structural configurations that distinguish the two phases, and the factors responsible for the energetic barrier occurring between the contrasting ''energy landscapes''.

References

1 G. Debenedetti Pablo, *Metastable liquids: concepts and principles*, Princeton University Press, Princeton, N.J., 1996.
2 Richard Zallen, *The physics of amorphous solids*, Wiley, New York, 1983.
3 Jean-Louis Barrat and Jean Pierre Hansen, *Basic concepts for simple and complex liquids*, Cambridge University Press, New York, 2003.
4 C. J. Benmore, R. T. Hart, Q. Mei, D. L. Price, J. Yarger, C. A. Tulk and D. D. Klug, *Phys. Rev. B: Condens. Matter Mater. Phys.*, 2005, **72**(13).
5 S. Biggin and J. E. Enderby, *J. Phys. C: Solid State Phys.*, 1981, **14**(22), 3129; J. A. E. Desa, A. C. Wright, J. Wong and R. N. Sinclair, *J. Non-Cryst. Solids*, 1982, **51**(1), 57; S. R. Elliott, *Nature*, 1991, **354**(6353), 445; S. R. Elliott, *Phys. Rev. Lett.*, 1991, **67**(6), 711; D. L. Price, A. J. G. Ellison, M. L. Saboungi, R. Z. Hu, T. M. Egami and W. S. Howells, *Phys. Rev. B: Condens. Matter*, 1997, **55**(17), 11249; P. S. Salmon, *Proc. R. Soc. London, Ser. A*, 1994, **445**(1924), 351.
6 P. S. Salmon, R. A. Martin, P. E. Mason and G. J. Cuello, *Nature*, 2005, **435**(7038), 75.
7 D. L. Price, *Curr. Opin. Solid State Mater. Sci.*, 1996, **1**(4), 572.
8 H. E. Fischer, A. C. Barnes and P. S. Salmon, *Rep. Prog. Phys.*, 2006, **69**(1), 233.
9 H. E. Fischer, P. S. Salmon and A. C. Barnes, *J. Phys. I*, 2003, **103**, 359.
10 P. A. Madden and M. Wilson, *Chem. Soc. Rev.*, 1996, **25**(5), 339 ff.
11 C. A. Angell, *Science*, 1995, **267**(5206), 1924.
12 C. Austen Angell and Martin Goldstein*Dynamic aspects of structural change in liquids and glasses*, New York Academy of Sciences, New York, N.Y., 1986.
13 F. H. Stillinger, *Science*, 1995, **267**(5206), 1935.
14 P. F. McMillan, in *High pressure phenomena: proceedings of the International School of Physics ''Enrico Fermi'': course CXLVII:Varenna on Como Lake, Villa Monastero, 3–13 July 2001*, ed. Russell J. Hemley, G. L. Chiarotti and M. Bernasconi, IOS Press; Ohmsha, Amsterdam, Washington D.C., Tokyo, Japan, 2002, p. xxix; P. F. McMillan, *Curr. Opin. Solid State Mater. Sci.*, 1999, **4**(2), 171; P. F. McMillan, *High Pressure Res.*, 2003, **23**(1–2), 7; P. F. McMillan and D. C. Clary, *Philos. Trans. R. Soc. London, Ser. A*, 2005, **363**(1827), 311.
15 G. H. Wolf, S. Wang, C. A. Herbst,D. J. Durban,W. F. Oliver, Z. C. Zang and K. Halvorson, in *High-pressure research: application to earth and planetary sciences*, ed. Yasuhiko Syono and M. H. Manghnani, Terra Scientific Pub. Co., American Geophysical Union, Tokyo, Washington, D.C., 1992, p. 503.
16 D. L. Price, S. C. Moss, R. Reijers, M. L. Saboungi and S. Susman, *J. Phys. C: Solid State Phys.*, 1988, **21**(32), L1069.
17 M. Grimsditch, *Phys. Rev. B: Condens. Matter*, 1986, **34**(6), 4372; P. F. McMillan, in *High pressure phenomena: proceedings of the International School of Physics ''Enrico Fermi'': course CXLVII:Varenna on Como Lake, Villa Monastero, 3–13 July 2001*, ed. R. J. Hemley, G. L. Chiarotti and M. Bernasconi, IOS Press, Ohmsha, Amsterdam, Washington D.C. Tokyo, Japan, 2002, p. 511.
18 M. Grimsditch, *Phys. Rev. Lett.*, 1984, **52**(26), 2379.
19 D. J. Wales, J. P. K. Doye, M. A. Miller, P. N. Mortenson, T. R. Walsh, G. B. McMillan and S. W. Martin, *Adv. Chem. Phys.*, 2000, **115**(115), 1; D. J. Wales, *Energy landscapes*, Cambridge University Press, Cambridge, UK, New York, 2003.
20 P. H. Poole, T. Grande, C. A. Angell and P. F. McMillan, *Science*, 1997, **275**(5298), 322.
21 C. A. Angell and C. T. Moynihan, *Metall. Mater. Trans. B*, 2000, **31**(4), 587.
22 C. A. Angell, K. L. Ngai, G. B. McKenna, P. F. McMillan and S. W. Martin, *J. Appl. Phys.*, 2000, **88**(6), 3113.
23 P. G. Debenedetti, F. H. Stillinger and M. S. Shell, *J. Phys. Chem. B*, 2003, **107**(51), 14434.
24 V. V. Brazhkin, S. V. Popova and R. N. Voloshin, *Physica B (Amsterdam)*, 1999, **265**(1–4), 64.
25 Y. Katayama, *J. Non-Cryst. Solids*, 2002, **312**, 8.
26 G. D. Mukherjee, S. N. Vaidya and V. Sugandhi, *Phys. Rev. Lett.*, 2001, **87**(19), 195501.
27 V. V. Brazhkin, S. V. Buldyrev and V. N. Rhzhov and H. E. Stanley, *New kinds of phase transitions: transformations in disordered substances*, Kluwer Academic Publishers, Dordrecht, Boston, 2002.
28 Y. Katayama, T. Mizutani, W. Utsumi, O. Shimomura, M. Yamakata and K. Funakoshi, *Nature*, 2000, **403**(6766), 170.
29 O. Mishima, L. D. Calvert and E. Whalley, *Nature*, 1984, **310**(5976), 393.
30 E. Rapaport, *J. Chem. Phys.*, 1968, **48**(4), 1433.
31 V. V. Brazhkin, S. V. Demishev, Y. V. Kosichkin, D. G. Lunts, A. G. Lyapin, S. V. Popova, N. E. Sluchanko and S. V. Frolov, *Zh. Eksp. Teor. Fiz.*, 1993, **104**(3), 3126; V. V. Brazhkin, R. N. Voloshin and S. Popova and A. Lyapin, in *New kinds of phase transitions: transformations in disordered substances. NATO science series. Series II, Mathematics, physics, and chemistry*, ed. V. V. Brazhkin, S. V. Buldyrev, V. N. Rhzhov and H. E. Stanley, Kluwer Academic Publishers, Dordrecht, Boston, 2002, Vol. 81, p. 239.
32 V. V. Brazhkin, D. R. Dmitriev and R. N. Voloshin, *Phys. Lett. A*, 1994, **193**(1), 102; V. V. Brazhkin, A. G. Lyapin, S. V. Popova and A. V. Sapelkin, *JETP Lett. Engl. Trans.*, 1994, **59**(2), 130.
33 V. V. Brazhkin and A. G. Lyapin, *J. Phys.: Condens. Matter*, 2003, **15**(36), 6059.
34 Y. Katayama and K. Tsuji, *J. Phys.: Condens. Matter*, 2003, **15**(36), 6085.
35 P. W. Bridgman, *Rev. Mod. Phys.*, 1946, **18**(1), 1; P. W. Bridgman, *Phys. Rev.*, 1947, **72**(6), 533.
36 Y. Le Godec, M. T. Dove, S. A. T. Redfern, M. G. Tucker, W. G. Marshall, G. Syfosse and S. Klotz, *High Pressure Res.*, 2003, **23**(3), 281; J. S. Loveday and R. J. Nelmes, *High Pressure Res.*, 2003, **23**(1–2), 41.
37 Y. Le Godec, T. Strassle, G. Hamel, R. J. Nelmes, J. S. Loveday, W. G. Marshall and S. Klotz, *High Pressure Res.*, 2004, **24**(1), 205.

38 J. Neuefeind, *J. Mol. Liq.*, 2002, **98–9**, 87.
39 A. Filipponi, *J. Phys.: Condens. Matter*, 2001, **13**(7), R23.
40 A. Filipponi, A. Di Cicco, S. De Panfilis, A. Trapananti, J. P. Itie, M. Borowski and S. Ansell, *J. Synchrotron Radiat.*, 2001, **8**, 81.
41 A. C. Wright, R. A. Hulme and R. N. Sinclair, *Phys. Chem. Glasses*, 2005, **46**(2), 59.
42 A. G. Kalampounias, S. N. Yannopoulos and G. N. Papatheodorou, *J. Chem. Phys.*, 2006, **124**(1); S. N. Yannopoulos, A. G. Kalampounias, A. Chrissanthopoulos and G. N. Papatheodorou, *J. Chem. Phys.*, 2003, **118**(7), 3197.
43 J. S. Loveday, R. J. Nelmes, W. G. Marshall, J. M. Besson, S. Klotz, G. Hamel and S. Hull, *High Pressure Res.*, 1996, **14**(4–6), 303.
44 M. Guthrie, C. A. Tulk, C. J. Benmore, J. Xu, J. L. Yarger, D. D. Klug, J. S. Tse, H. K. Mao and R. J. Hemley, *Phys. Rev. Lett.*, 2004, **93**(11), art. no-115502.
45 S. Sampath, C. J. Benmore, K. M. Lantzky, J. Neuefeind, K. Leinenweber, D. L. Price and J. L. Yarger, *Phys. Rev. Lett.*, 2003, **90**(11), 115502.
46 A. M. Saitta, T. Strassle, G. Rousse, G. Hamel, S. Klotz, R. J. Nelmes and J. S. Loveday, *J. Chem. Phys.*, 2004, **121**(17), 8430.
47 P. S. Salmon, *Nat. Mater.*, 2002, **1**(2), 87.
48 G. N. Greaves, *J. Non-Cryst. Solids*, 1985, **71**(1–3), 203; G. N. Greaves and E. A. Davis, *Philos. Mag.*, 1974, **29**(5), 1201; G. N. Greaves, A. Fontaine, P. Lagarde, D. Raoux and S. J. Gurman, *Nature*, 1981, **293**(5834), 611; A. C. Wright, *J. Non-Cryst. Solids*, 1985, **75**(1–3), 15; A. C. Wright, G. A. N. Connell and J. W. Allen, *J. Non-Cryst. Solids*, 1980, **42**(1–3), 69; A. C. Wright, R. A. Hulme, D. I. Grimley, R. N. Sinclair, S. W. Martin, D. L. Price and F. L. Galeener, *J. Non-Cryst. Solids*, 1991, **129**(1–3), 213.
49 R. L. McGreevy, *J. Phys.: Condens. Matter*, 2001, **13**(46), R877.
50 A. K. Soper, *Phys. Rev. B: Condens. Matter Mater. Phys.*, 2005, **72**(10).
51 M. P. Allen and D. J. Tildesley, *Computer simulation of liquids*, Clarendon Press, Oxford University Press, Oxford, New York, 1987.
52 W. D. Luedtke and U. Landman, *Phys. Rev. B: Condens. Matter*, 1988, **37**(9), 4656.
53 M. Wilson and P. F. McMillan, *Phys. Rev. B: Condens. Matter Mater. Phys.*, 2004, **69**(5).
54 M. Wilson and P. F. McMillan, *Phys. Rev. Lett.*, 2003, **90**(13), 135703.
55 P. Richet and P. Gillet, *Eur. J. Mineral.*, 1997, **9**(5), 907.
56 E. Rapaport, *J. Chem. Phys.*, 1967, **46**(8), 2891.
57 O. Mishima, L. D. Calvert and E. Whalley, *Nature*, 1985, **314**(6006), 76.
58 E. Whalley, O. Mishima and Y. P. Handa and D. D. Klug, in *Dynamic aspects of structural change in liquids and glasses*, ed. C. Austen Angell and Martin Goldstein, New York Academy of Sciences, New York, N.Y., 1986, Vol. 484, p. ix.
59 E. A. Guggenheim, *Modern thermodynamics by the methods of Willard Gibbs*, Methuen & co. ltd., London, 1933.
60 E. G. Ponyatovsky, V. V. Sinitsyn and T. A. Pozdnyakova, *J. Chem. Phys.*, 1998, **109**(6), 2413.
61 C. T. Moynihan, *Mater. Res. Soc. Proc.*, 1997, **455**, 411.
62 E. G. Ponyatovsky, I. T. Belash and O. I. Barkalov, *J. Non-Cryst. Solids*, 1990, **117**, 679.
63 C. A. Angell, C. T. Moynihan and M. Hemmati, *J. Non-Cryst. Solids*, 2000, **274**(1–3), 319.
64 D. R. Uhlmann, *J. Non-Cryst. Solids*, 1980, **38–9**(MAY-), 693; D. R. Uhlmann, *Am. Ceram. Soc. Bull.*, 1979, **58**(3), 384; D. R. Uhlmann, *J. Non-Cryst. Solids*, 1977, **25**(1–3), 42.
65 C. T. Moynihan and C. A. Angell, *J. Non-Cryst. Solids*, 2000, **274**(1–3), 131.
66 O. Mishima, *J. Chem. Phys.*, 1994, **100**(8), 5910.
67 A. Ha, I. Cohen, X. L. Zhao, M. Lee and D. Kivelson, *J. Phys. Chem.*, 1996, **100**(1), 1; D. Kivelson and G. Tarjus, *J. Non-Cryst. Solids*, 2002, **307**, 630.
68 A. Hedoux, T. Denicourt, Y. Guinet, L. Carpentier and M. Descamps, *Solid State Commun.*, 2002, **122**(7–8), 373.
69 A. Hedoux, J. Dore, Y. Guinet, M. C. Bellissent-Funel, D. Prevost, M. Descamps and D. Grandjean, *Phys. Chem. Chem. Phys.*, 2002, **4**(22), 5644.
70 D. J. Lacks, *Phys. Rev. Lett.*, 2000, **84**(20), 4629.
71 S. Aasland and P. F. McMillan, *Nature*, 1994, **369**(6482), 633.
72 M. C. Wilding, M. Wilson and P. F. McMillan, *Philos. Trans. R. Soc. London, Ser. A*, 2005, **363**(1827), 589.
73 M. C. Wilding and P. F. McMillan, in *New kinds of phase transitions: transformations in disordered substances*, ed. V. V. Brazhkin, S. V. Buldyrev, V. N. Rhzhov and H. E. Stanley, Kluwer Academic Publishers, Dordrecht, Boston, 2002, pp. 57.
74 M. C. Wilding, C. J. Benmore and P. F. McMillan, *J. Non-Cryst. Solids*, 2002, **297**(2–3), 143.
75 H. Tanaka, *Phys. Rev. E*, 2000, **62**(5 Part B), 6968.
76 H. Tanaka, *Europhys. Lett.*, 2000, **50**(3), 340; H. Tanaka, R. Kurita and H. Mataki, *Phys. Rev. Lett.*, 2004, **9202**(2), 5701.
77 C. A. Angell, S. Borick and M. Grabow, *J. Non-Cryst. Solids*, 1996, **207**(Part 2), 463; M. Hemmati, C. T. Moynihan and C. A. Angell, *J. Chem. Phys.*, 2001, **115**(14), 6663.
78 O. Mishima and H. E. Stanley, *Nature*, 1998, **396**(6709), 329; O. Mishima and Y. Suzuki, *Nature*, 2002, **419**(6907), 599; O. Mishima, K. Takemura and K. Aoki, *Science*, 1991, **254**(5030), 406.
79 M. C. Bellissent-Funel, *Nuovo Cimento della Societa Italiana di Fisica D-Condensed Matter Atomic Molecular & Chemical Physics Fluids Plasmas Biophysics*, 1998, **20**(12BIS), 2107; M. C. Bellissent-Funel, *Europhys. Lett.*, 1998, **42**(2), 161; M. A. Ricci and A. K. Soper, *Physica A*, 2002, **304**(1–2), 43; A. K. Soper, *Chem. Phys.*, 1984, **88**(1), 187.
80 A. K. Soper, *Physica B+C*, 1986, **136**(1–3), 322; A. K. Soper, *Science*, 2002, **297**(5585), 1288.
81 A. H. Narten and R. L. Hahn, *Science*, 1982, **217**(4566), 1249; A. H. Narten, W. E. Thiessen and L. Blum, *Science*, 1982, **217**(4564), 1033.
82 C. A. Angell, *Philos. Trans. R. Soc. London, Ser. A*, 2005, **363**(1827), 415.
83 A. K. Soper, *Chem. Phys.*, 2000, **258**(2–3), 121.
84 A. K. Soper, *Mol. Phys.*, 2001, **99**(17), 1503.
85 D. D. Klug, *Phys. World*, 2005, **18**(2), 25; D. D. Klug, C. A. Tulk, E. C. Svensson and C. K. Loong, *Abstr. Pap. Am. Chem. Soc.*, 1999, **218**, U298.
86 J. L. Finney, A. Hallbrucker, I. Kohl, A. K. Soper and D. T. Bowron, *Phys. Rev. Lett.*, 2002, **88**(22), 225503.
87 A. K. Soper and M. A. Ricci, *Phys. Rev. Lett.*, 2000, **84**(13), 2881.
88 J. L. Finney, D. T. Bowron, A. K. Soper, T. Loerting, E. Mayer and A. Hallbrucker, *Phys. Rev. Lett.*, 2002, **89**(20), 205503.
89 M. Guthrie, C. A. Tulk, C. J. Benmore and D. D. Klug, *Chem. Phys. Lett.*, 2004, **397**(4–6), 335.
90 H. E. Stanley, S. V. Buldyrev, N. Giovambattista E. La Nave, A. La Scala, F. Sciortino, F. W. Starrin *New kinds of phase transitions: transformations in disordered substances*, ed. V. V. Brazhkin, S. V. Buldyrev, V. N. Rhzhov and H. E. Stanley, Kluwer Academic Publishers, Dordrecht, Boston, 2002, p. 309.
91 H. E. Stanley, S. V. Buldyrev, O. Mishima, M. R. Sadr-Lahijany, A. Scala and F. W. Starr, *J. Phys.: Condens. Matter*, 2000, **12**(8A), A403.
92 S. Klotz, G. Hamel, J. S. Loveday, R. J. Nelmes, M. Guthrie and A. K. Soper, *Phys. Rev. Lett.*, 2002, **89**(28).
93 C. A. Tulk, C. J. Benmore, J. Urquidi, D. D. Klug, J. Neuefeind, B. Tomberli and P. A. Egelstaff, *Science*, 2002, **297**(5585), 1320.
94 M. Guthrie, J. Urquidi, C. A. Tulk, C. J. Benmore, D. D. Klug and J. Neuefeind, *Phys. Rev. B: Condens. Matter Mater. Phys.*, 2003, **68**(18), art. no.-184110.
95 S. Klotz, T. Strassle, A. M. Saitta, G. Rousse, G. Hamel, R. J. Nelmes, J. S. Loveday and M. Guthrie, *J. Phys.: Condens. Matter*, 2005, **17**(11), S967.
96 S. K. Deb, M. Wilding, M. Somayazulu and P. F. McMillan, *Nature*, 2001, **414**(6863), 528.
97 P. F. McMillan, M. Wilson, D. Daisenberger and D. Machon, *Nat. Mater.*, 2005, **4**(9), 680.
98 S. Sastry and C. A. Angell, *Nat. Mater.*, 2003, **2**(11), 739.
99 G. Monaco, S. Falconi, W. A. Crichton and M. Mezouar, *Phys. Rev. Lett.*, 2003, **90**(25), 255701.
100 Y. Senda, F. Shimojo and K. Hoshino, *J. Non-Cryst. Solids*, 2002, **312**, 80.
101 M. C. Wilding, P. F. McMillan and A. Navrotsky, *Phys. Chem. Glasses*, 2003, **43**(6), 306; M. C. Wilding, P. F. McMillan and A. Navrotsky, *Physica A*, 2002, **314**(1–4), 379.

102 J. K. R. Weber, J. A. Tangeman, T. S. Key and P. C. Nordine, *J. Thermophys. Heat Transfer*, 2003, **17**(2), 182.
103 M. Wilson and P. F. McMillan, *Phys. Rev. B: Condens. Matter Mater. Phys.*, 2004, **6905**(5), 4206.
104 S. Sampath, C. J. Benmore, K. M. Lantzky, J. Neuefeind, K. Leinenweber, D. L. Price and J. L. Yarger, *Phys. Rev. Lett.*, 2003, **90**(11).
105 P. S. Salmon and S. Q. Xin, *Phys. Rev. B: Condens. Matter Mater. Phys.*, 2002, **65**(6).
106 E. Bychkov, C. J. Benmore and D. L. Price, *Phys. Rev. B: Condens. Matter Mater. Phys.*, 2005, **72**(17).
107 P. S. Salmon and I. Petri, *J. Phys.: Condens. Matter*, 2003, **15**(16), S1509.
108 M. Durandurdu and D. A. Drabold, *Phys. Rev. B: Condens. Matter Mater. Phys.*, 2002, **65**(10), 104208; M. Cobb and D. A. Drabold, *Phys. Rev. B: Condens. Matter*, 1997, **56**(6), 3054; M. Cobb, D. A. Drabold and R. L. Cappelletti, *Phys. Rev. B: Condens. Matter*, 1996, **54**(17), 12162.
109 W. A. Crichton and N. L. Ross, *Mineral. Mag.*, 2005, **69**(3), 273.
110 S. Stolen, T. Grande and H. B. Johnsen, *Phys. Chem. Chem. Phys.*, 2002, **4**(14), 3396.
111 Q. Mei, C. Benmore, R. T. Hart, E. Bychkov, P. S. Salmon, C. D. Martin, F. M. Michel, Y. V. Antonov, P. J. Chupas, P. L. Lee, S. D. Shastri, J. B. Parise, K. Leinenweber, S. Amin and J. Larger, *Phys. Rev. B: Condens. Matter Mater. Phys.*, 2006, 74.
112 F. Wang, S. Mamedov, P. Boolchand, B. Goodman and M. Chandrasekhar, *Phys. Rev. B: Condens. Matter Mater. Phys.*, 2005, **71**(17).
113 Q. Mei, P. V. Teredesai, C. J. Benmore, S. Sampath, J. L. Yarger, E. Bychkov, J. Neuefeind and K. Lienenweber, *Phys. Chem. Glasses*, 2005, **46**(4), 483.
114 W. A. Crichton, M. Mezouar, T. Grande, S. Stolen and A. Grzechnik, *Nature*, 2001, **414**(6864), 622.
115 A. Hedoux, Y. Guinet and M. Descamps, *Phys. Rev. B: Condens. Matter Mater. Phys.*, 1998, **58**(1), 31.
116 R. Kurita and H. Tanaka, *Phys. Rev. B: Condens. Matter Mater. Phys.*, 2006, **73**(10).
117 H. Tanaka, R. Kurita and H. Mataki, *Phys. Rev. Lett.*, 2004, **92**(2).
118 C. Alba-Simionesco and G. Tarjus, *Europhys. Lett.*, 2000, **52**(3), 297.
119 P. H. Poole, F. Sciortino, U. Essmann and H. E. Stanley, *Nature*, 1992, **360**(6402), 324; P. H. Poole, S. Harrington, F. Sciortino and H. E. Stanley, *Nuovo Cimento della Societa Italiana di Fisica D-Condensed Matter Atomic Molecular & Chemical Physics Fluids Plasmas Biophysics*, 1998, **20**(12BIS), 2143.
120 N. B. Wilding and J. E. Magee, *Physical Review E*, 2002, **66**(3).
121 P. A. Egelstaff, *An introduction to the liquid state*, Academic Press, London, New York, 1967.
122 P. G. Debenedetti and F. H. Stillinger, *Nature*, 2001, **410**, 259.

